

Hierarchical Quantized Federated Learning: Convergence Analysis and System Design

Lumin Liu, *Student Member, IEEE*, Jun Zhang, *Senior Member, IEEE*,
Shenghui Song, *Member, IEEE*, and Khaled B. Letaief, *Fellow, IEEE*

Abstract

Federated learning is a collaborative machine learning framework to train deep neural networks without accessing clients' private data. Previous works assume one central parameter server either at the cloud or at the edge. A cloud server can aggregate knowledge from all participating clients but suffers high communication overhead and latency, while an edge server enjoys more efficient communications during model update but can only reach a limited number of clients. This paper exploits the advantages of both cloud and edge servers and considers a Hierarchical Quantized Federated Learning (HQFL) system with one cloud server, several edge servers and many clients, adopting a communication-efficient training algorithm, Hier-Local-QSGD. The high communication efficiency comes from frequent local aggregations at the edge servers and fewer aggregations at the cloud server, as well as weight quantization during model uploading. A tight convergence bound for non-convex objective loss functions is derived, which is then applied to investigate two design problems, namely, the accuracy-latency trade-off and edge-client association. It will be shown that given a latency budget for the whole training process, there is an optimal parameter choice with respect to the two aggregation intervals and two quantization levels. For the edge-client association problem, it is found that the edge-client association strategy has no impact on the convergence speed. Empirical simulations shall verify the findings from the convergence analysis and demonstrate the accuracy-latency trade-off in the hierarchical federated learning system.

Index Terms

Federated Learning, Mobile Edge Computing, Convergence Analysis, Local SGD.

Part of the results was presented at the IEEE International Conference on Communications (ICC), 2020 [1]. L. Liu, S. H. Song and K.B. Letaief are with the Department of Electronic and Computer Engineering, Hong Kong University of Science and Technology, Hong Kong (Email: lliubb, eeshsong, eekhaled@ust.hk). J. Zhang is with the Department of Electronic and Information Engineering, The Hong Kong Polytechnic University, Hong Kong (E-mail: jun-eie.zhang@polyu.edu.hk).

I. INTRODUCTION

Deep Learning (DL) has revolutionized many application areas during the past few years, such as image processing, natural language processing, and video analytics [2]. The conventional way of training a high-quality DL model is based on a centralized approach, e.g., in a cloud data center with massive data samples. However, in many practical scenarios, data are generated and maintained at end devices, such as smartphones. As a result, moving them to a central server for model training will lead to excessive communication overhead and may also violate privacy. Federated Learning (FL) [3] is one of the most promising frameworks for privacy-preserving DL. With FL, model training happens at the clients and only the trained models are required to be aggregated at the server, thus eliminating the need for sharing private user data. Its feasibility has been verified in real-world applications, e.g., the Google keyboard prediction [4].

Given the increasing size of the DL models and frequent communication between the clients and server, communication efficiency is among the most important issues in FL. FL enables fully distributed training by decomposing the process into two recurring steps, i.e., parallel model update based on local data at the clients and then global model aggregation at the server. Due to the privacy regulation, the local data generated by different users reside on mobile devices with unstable, limited communication bandwidth and battery. While most studies on FL assumed a cloud server as the parameter server and adopted model quantization to reduce the communication overhead [5], [6], some recent works [7], [8] proposed to utilize edge servers to reduce communication latency and leverage Mobile Edge Computing (MEC) platforms [9]. This is often referred as Federated Edge Learning (FEL) [10], which enables learning a DL model at the network edge to support ultra-low latency applications [11], [12]. Although edge-based FL enjoys a lower round-trip latency, the number of clients that can participate the training decreases, which degrades the training performance. Thus, the selection between the cloud server and the edge server represents a trade-off between round-trip latency and learning performance.

This trade-off motivates us to consider a hierarchical architecture for FL, which includes one cloud server, multiple edge servers and many clients. The illustrations of the edge-based, cloud-based and hierarchical FL are shown in Fig. 1a. Such a hierarchical architecture was firstly proposed in our previous work [1]. There are two levels of aggregation in hierarchical FL, namely, the efficient and parallel edge aggregation and the time-consuming cloud aggregation. It was shown in [1], both theoretically and empirically, that hierarchical FL has a higher

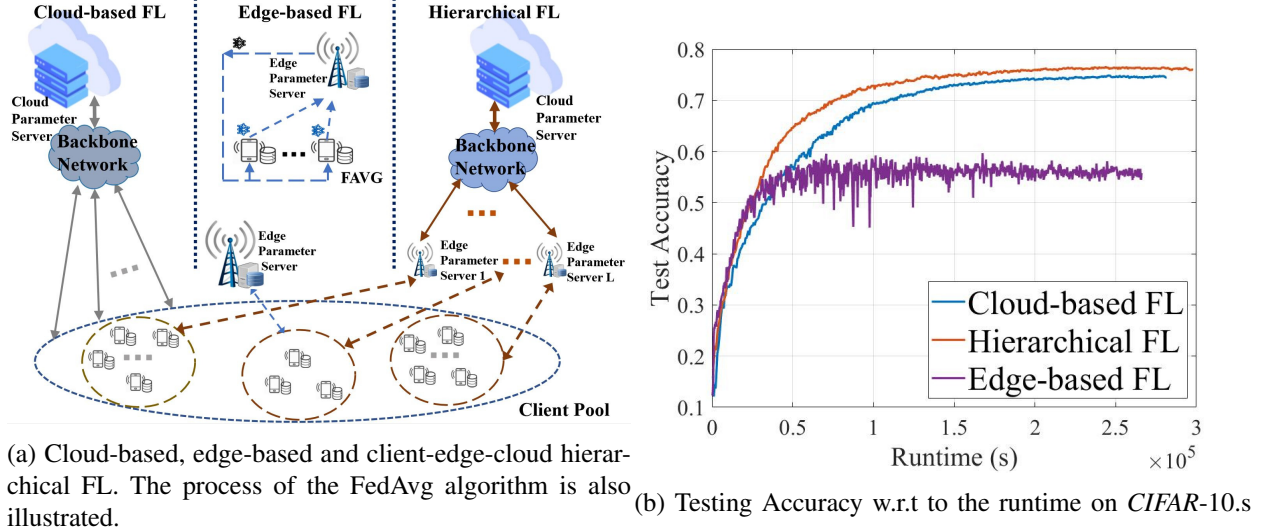


Fig. 1: Comparison of different FL frameworks.

convergence speed than the conventional two-layer FL. Furthermore, empirical experiments also have shown that the client-edge-cloud hierarchical architecture reduces training time and energy consumption compared with the single-server architecture, as illustrated in Fig. 1b. Driven by its great potentials, the hierarchical architecture has received much attention. These studies include the convergence analysis of the training algorithms [13], [14] and the design of an energy and time efficient hierarchical FL system with finite resources [15], [16]. Nevertheless, the theoretical understanding of hierarchical FL is far from complete. For example, the bound derived in [13] is loose for non-convex loss functions. The lack of tight convergence bound makes system design and optimization difficult. Besides, existing analyses [13], [14] are done assuming full-precision model updates, which leads to prohibitive communication overhead.

In this paper, we consider the hierarchical FL structure where model quantization is also adopted to further improve communication efficiency. With the proposed Hier-Local-QSGD algorithm, clients upload quantized updates periodically to their associated edge servers, and the edge servers upload quantized updates to the cloud server after several rounds of edge aggregation. We provide a tight convergence analysis of the Hier-Local-QSGD algorithm with non-convex loss functions in FL. The derived convergence bound is further utilized for system optimization in the areas of the accuracy-latency trade-off and the edge-client association problem. To the best of our knowledge, this is the first analytical result for hierarchical FL architecture with model quantization, which we refer to as HQFL, i.e., Hierarchical Quantized Federated Learning.

A. Contributions

We summarize the contributions of the paper as follows:

- 1) Based on the Client-Edge-Cloud hierarchical FL framework in [1], we propose a Hier-Local-QSGD algorithm, where each client uploads its compressed model updates periodically to its associated edge server and the edge servers upload compressed updates to the cloud server after several rounds of edge aggregation.
- 2) We provide a tight convergence analysis for the Hier-Local-QSGD algorithm for non-convex loss functions. The result is tighter than the best known result in literature [13] and the first to consider update quantization in hierarchical FL.
- 3) The convergence bound is utilized for system optimization in two areas, i.e., accuracy-latency trade-off and edge-client association. We show that different accuracy-latency trade-offs can be achieved by optimizing system parameters. On the other hand, the theoretical result also indicate that in the edge-client association problem, the convergence speed with respect to (w.r.t.) iterations is irrelevant to the edge-client association scheme, which significantly reduces the complexity.
- 4) We verify the findings from the theoretical analysis and demonstrate the accuracy-latency trade-offs through empirical results with two typical datasets, i.e. MNIST [17] and CIFAR-10 [18].

The paper is organized as follows. In Section II, related works in FL will be surveyed. In Section III, we will introduce the learning problem in FL, the hierarchical FL system, and the corresponding Hier-Local-QSGD algorithm. In Section IV, we will present the convergence analysis with a sketch of the proof. A detailed proof can be found in the appendix. In Section V, we discuss two applications in hierarchical FL, i.e., accuracy-latency trade-off and edge-client association. In Section VI, empirical results, as applied on two datasets, are demonstrated.

II. RELATED WORKS

FL has received massive attentions due to its great potentials in collaboratively training an ML model in a privacy-preserving way. Nevertheless, the initial proposal of the FL system along with the FedAvg algorithm in [3] was far from satisfactory for practical implementation, where the system scale can be colossal, and the communication and computation conditions of devices can be extremely unbalanced. Besides, privacy regulations in FL restrict the local training data from being reshuffled randomly from time to time to guarantee an independent and

identical data distribution (IID), which is a key assumption to facilitate the analysis of centralized training. Thus, the assurance of a successfully trained model is missing. Aiming to guarantee the effectiveness and efficiency of the FL system, works on the convergence analysis and resource allocation sprung up.

To ensure the effectiveness of model training in FL, many works analyzed the convergence of the FL training algorithm in a single-server FL for both convex and non-convex loss functions, starting from the simple case with the IID data distribution. With IID data, FedAvg could be seen as a direct extension of decentralized Stochastic Gradient Descent (SGD) [19] with multiple steps of SGD performed on the local data. Thus, the training algorithm is often referred to as *local SGD* [20]. The analysis of *local SGD* was performed in [20], [21] for convex loss functions and in [22] for non-convex loss functions. In [21], [22], the additional error term caused by multiple local updates was shown to grow linearly with the aggregation interval for the first time. In [6], the convergence of the FedAvg algorithm considering random client selection and update quantization was investigated. However, the statistical heterogeneity in FL failed to meet the IID data assumption, and experimental works [23] indeed showed the insufficiency of the analysis with the ideal IID assumption. Following works in [24], [21] relaxed the IID data assumption and demonstrated that the non-IID data distribution will cause an error term which is more sensitive to the local update interval than that under the IID assumption when using the FedAvg training algorithm.

Resource allocation is deemed as an effective method to improve the energy and time efficiency of FL system. Current research on resource allocation in FL mainly focused on the following three aspects, namely, spectrum allocation, power control [7], and local aggregation interval control [8], [25]. In these works, the resource allocation problem is formulated as an optimization problem to minimize the latency or the energy of the FL system subject to the constraint of obtaining a good model with a desired accuracy. Tight convergence results play a critical role to formulate such resource allocation problems.

For hierarchical FL, the convergence analysis has been less well studied with many still interesting open problems. Our previous work [1] analyzed the convergence of hierarchical FL with both convex and non-convex loss functions and non-IID data. However, the optimizer at the client side is a full-batch gradient descent, which may not be practical for devices with a limited computation ability. In [13], the authors provided a convergence analysis of hierarchical FL for non-convex loss functions with the IID data assumption, where the obtained error bound

TABLE I: Key Notations

Symbol	Definitions	Symbol	Definitions
x	$x \in \mathbb{R}^P$, vector of the learning model	C^ℓ	The set of the clients under edge ℓ
\mathcal{P}	The joint underlying probability distribution of the input space and output space	τ_2	The edge-cloud aggregation interval
ξ	$\xi \in \mathbb{R}^u$, a random variable with an unknown probability distribution \mathcal{P}	τ_1	The client-edge aggregation interval
\mathcal{L}	$\mathbb{R}^P \times \mathbb{R}^u \rightarrow \mathbb{R}$, a stochastic loss function associated with the learning objective	k	The index of the cloud aggregation step
ξ_i	A realization from the unknown distribution \mathcal{P}	t_2	The index of the edge-aggregation step, $0 \leq t_2 < \tau_2$
\mathcal{D}	$\mathcal{D} = \{\xi_i\}_{i=1}^D$, the set of the realizations, a.k.a, train dataset, D is the size of the training dataset	t_1	The index of the client local update step, $0 \leq t_1 < \tau_1$
n	The number of participated clients in the whole hierarchical FL system	x_{k,t_1,t_2}^i	Local model parameters on client i at step (k, t_2, t_1)
s	The number edge servers in the whole system	x_k	Cloud model parameters after k -th cloud aggregation step
m^ℓ	The number of participated clients under edge parameter server ℓ	u_{k,t_2}^ℓ	Edge model parameters on edge ℓ after t_2 -th edge aggregation in the k -th cloud aggregation interval

is quadratic with the aggregation interval and is loose. Later, a tighter error bound was provided in [14] for non-convex loss functions with non-IID data. The analyses done in [13], [14] both consider full-precision model updates. In addition to the theoretical convergence analysis, [15] considered the edge-client association problem in the hierarchical FL.

III. SYSTEM DESCRIPTION

In this section, we will introduce the FL learning problem considered in this paper. The standard single-server FL system and its algorithm will be briefly reviewed for the sake of completeness. We will then introduce the hierarchical FL system and the Hier-Local-QSGD algorithm, with one cloud server, s edge servers and n users. Each client has an equally-sized training dataset \mathcal{D}_i and the edge-client association is denoted by the client set under edge server ℓ , i.e., C^ℓ . Other key notations that are important for the algorithm and the theoretical analysis are summarized in Table I.

A. Centralized Learning vs. Federated Learning

Before diving into the training problem formulation of FL, we will introduce some preliminaries of the problem formulation in centralized training. For supervised learning, the following

objective loss function is considered:

$$\min_x L(x) = \min_x \mathbb{E}_{\xi \sim \mathcal{P}} [\mathcal{L}(x, \xi)], \quad (1)$$

where \mathcal{P} denotes the joint distribution of the input and output space, ξ is a random variable generated from the distribution \mathcal{P} , x denotes the learning model parameter, and \mathcal{L} denotes the stochastic loss function associated with the learning objective, i.e., cross-entropy loss function for classification task, $L : \mathbb{R}^p \rightarrow \mathbb{R}$ denotes the expected loss function over the unknown probability distribution \mathcal{P} , and it is also called as the population risk. However, the data distribution \mathcal{P} is unknown and an empirical risk minimization (ERM) problem $f(x)$ is considered as the objective loss function to minimize in training the neural network model:

$$\min_x f(x) = \min_x \frac{1}{|\mathcal{D}|} \sum_{\xi_i \in \mathcal{D}} \mathcal{L}(x, \xi_i). \quad (2)$$

The generalization error, i.e., the difference between $L(x)$, the population risk function, and $f(x)$, the empirical risk function decreases with the number of training samples in the training data set \mathcal{D} [26], which theoretically supports the need of a massive training data set in Deep Learning.

The most commonly adopted optimization algorithm in centralized training is SGD or its variants [19]. Even though the objective loss function $f(x)$ is most likely to be non-convex, the simple Gradient Descent algorithm has shown its effectiveness, and its stochastic version has greatly improved the computing efficiency by sampling a small batch of data to compute the gradient. In centralized training, the model parameters evolve as follows:

$$x_t = x_{t-1} - \eta \tilde{\nabla} f(x_{t-1}), \quad (3)$$

where $\tilde{\nabla} f(x)$ is the gradient estimated based on a randomly sampled data point ξ from the training data set \mathcal{D} , and η is the learning rate of the algorithm, which is often a hyper parameter to be tuned in the training process.

For FL, the objective loss function to minimize is also the empirical risk over all the training data except that only the local training samples can be accessed for each user. Suppose that there are n clients with its dataset $\{\mathcal{D}_i\}$ of size D generated with the probability distribution $\{\mathcal{P}_i\}_{i=1}^n$.

Algorithm 1: Hierarchical Local SGD with Quantization (Hier-Local-QSGD)

Initialize the model on the cloud server x_0 ;

for $k = 0, 1, \dots, K - 1$ **do**

for $\ell = 1, \dots, s$ *edge servers in parallel* **do**

 Set the edge model same as the cloud server;

$u_{k,0}^\ell = x_k$;

for $t_2 = 0, 1, \dots, \tau_2 - 1$ **do**

for $i \in C^\ell$ *clients in parallel* **do**

 Set the clients model same as the associated edge server;

$x_{k,t_2,0}^i = u_{k,t_2}^\ell$;

for $t_1 = 0, 1, \dots, \tau_1 - 1$ **do**

$x_{k,t_2,t_1+1}^i = x_{k,t_2,t_1}^i - \eta \tilde{\nabla} f_i(x_{k,t_2,t_1}^i)$

end

 Send $\mathcal{Q}_1(x_{k,t_2\tau_1}^i - x_{k,t_2,0}^i)$ to its associated edge server

end

 Edge server aggregates the quantized updates from the clients;

$u_{k,t_2+1}^\ell = u_{k,t_2}^\ell + \frac{1}{m^\ell} \sum_{i \in \mathcal{D}^\ell} \mathcal{Q}_1(x_{k,t_2\tau_1}^i - x_{k,t_2,0}^i)$

end

 Send $\mathcal{Q}_2(u_{k,\tau_2}^\ell - u_{k,0}^\ell)$

end

 Cloud server aggregates the quantized updates from the edge servers;

$x_{k+1} = x_k + \sum_{\ell=1}^s \frac{m^\ell}{n} \mathcal{Q}_2(u_{k,\tau_2}^\ell - u_{k,0}^\ell)$

end

Based on the local dataset $\{\mathcal{D}_i\}$, we have the empirical local loss function for each user:

$$f_i(x) = \frac{1}{D} \sum_{\xi_j \in \mathcal{D}_i} \mathcal{L}(x, \xi_j). \quad (4)$$

The goal of the FL training algorithm is to learn a global model that performs well on the average of the local data distributions. Denote the joint dataset as $\mathcal{D} = \bigcup_{i=1}^n \mathcal{D}_i$, and the final loss function to minimize is:

$$f(x) = \frac{1}{nD} \sum_{\xi_j \in \mathcal{D}} \mathcal{L}(x, \xi_j) = \frac{1}{n} \sum_{i=1}^n f_i(x). \quad (5)$$

In this paper, we assume that the local data distributions are identical, i.e., $\mathcal{P}_i = \mathcal{P}$, $i = 1, \dots, n$, which guarantees that the stochastic gradient estimated based on local data set \mathcal{D}_i in expectation equals to the gradient estimated based on the global joint dataset \mathcal{D} .

B. Two-Layer FL and Hierarchical FL

In the following, we introduce the traditional two-layer FL system and hierarchical FL system along with its training algorithm.

In the traditional two-layer FL system, there is one central parameter server and n clients. Each client performs τ steps of SGD iterations locally and then uploads the model updates to the central parameter server. The central server averages the updates and redistributes the averaged outcomes back to each client. The process repeats itself until the model reaches a desired accuracy or due to limited resources, e.g., the energy or time budget run out.

The parameters of the local model on the i -th client after t steps of SGD iterations are denoted as x_t^i . In this case, x_t^i in the FedAvg algorithm evolves in the following way:

$$x_t^i = \begin{cases} x_{t-1}^i - \eta \tilde{\nabla} f_i(x_{t-1}^i) & t \mid \tau \neq 0 \\ \frac{1}{n} \sum_{i=1}^n [x_{t-1}^i - \eta \tilde{\nabla} f_i(x_{t-1}^i)] & t \mid \tau = 0 \end{cases} \quad (6)$$

In FedAvg, the model aggregation step can be interpreted as a way to exchange information among the clients. Thus, aggregation at a cloud parameter server can incorporate data from many clients, but the communication cost is high. On the other hand, aggregation at an edge parameter server only incorporates a small number of clients with a much cheaper communication cost.

To combine their advantages, we consider a hierarchical FL system, which has one cloud server, s edge servers indexed by ℓ , with disjoint client sets $\{C^\ell\}_{\ell=1}^s$, and n clients indexed by i and ℓ , with distributed datasets $\{\mathcal{D}_i^\ell\}_{i=1}^N$. The hierarchical FL system exploits the natural client-edge-cloud communication hierarchy in current communication networks.

With this hierarchical FL architecture, we propose a Hier-Local-QSGD algorithm as described in Algorithm 1. The key steps of the Hier-Local-QSGD algorithm include the following two modules to improve communication efficiency.

1) Frequent Edge Aggregation and Infrequent Cloud Aggregation: Periodic aggregation is the key step in reducing the communication cost in FL. A larger aggregation interval reduces the communication rounds given a fixed number of SGD iterations. But a large τ will also degrade the performance of the obtained DL model after a fixed number of SGD iterations. This is because too many steps of local SGD updates will lead the local models to approach the optima of the local loss function $f_i(x)$ instead of the global loss function $f(x)$.

Edge aggregation has a lower propagation latency compared with cloud aggregation. Hence,

each edge server can efficiently aggregate the models within its local area for several times before the cloud aggregation. To be more specific, after every τ_1 local SGD updates on each client, each edge server averages its clients' models. After every τ_2 edge model aggregations, the cloud server then averages all the edge servers' models. Thus, the communication with the cloud happens every $\tau_1\tau_2$ local updates. In this way, the local model is less likely to be biased towards its local minima compared with the case in FedAvg with an aggregation interval of $\tau = \tau_1\tau_2$.

2) **Quantized Model Updates:** The overall communication cost in FL also depends on the DL model size, which determines the amount of data to be transmitted in each communication round. Quantization is often used to reduce the size of the model updates. A trade-off exists in quantization. A low-precision quantizer reduces the communication overhead but also introduces additional noise during the training process, which will ultimately degrade the trained model performance. Thus, investigating the effect of the quantization is important.

We give an example of a widely-used random quantizer.

Example 1 (Random Sparsification) Fix $r \in 1, \dots, d$ and let $\zeta \in \mathbb{R}^d$ be a (uniformly distributed) random binary vector with r non-zero entries. The random sparsification operator is given by:

$$Q(x) = \frac{d}{r} (\zeta \odot x)$$

where \odot denotes the Hadamard (entry-wise) product.

We use Q_1, Q_2 to represent the quantizers applied on the model updates from the client to the edge server and the model updates from the edge servers to the cloud server, respectively.

The comparison between FedAvg and *Hier-Local-SGD* is illustrated in Fig. 2. Details of the Hier-Local-QSGD algorithm are presented in Algorithm 1. The local model parameters after k rounds of cloud aggregation, t_2 rounds of edge-aggregation and t_1 steps of local update on client i are denoted by x_{k,t_2,t_1} . We will use the tuple (k, t_2, t_1) to denote the local iteration step throughout the paper. Specifically, the steps of local iterations t can be expressed as: $t = k\tau_1\tau_2 + t_2\tau_1 + t_1$. Similarly, model parameters on edge ℓ after k rounds of cloud aggregation and t_2 rounds of edge aggregation are denoted by u_{k,t_2}^ℓ , model parameters on the cloud server after k rounds of cloud aggregation are denoted by x_k .

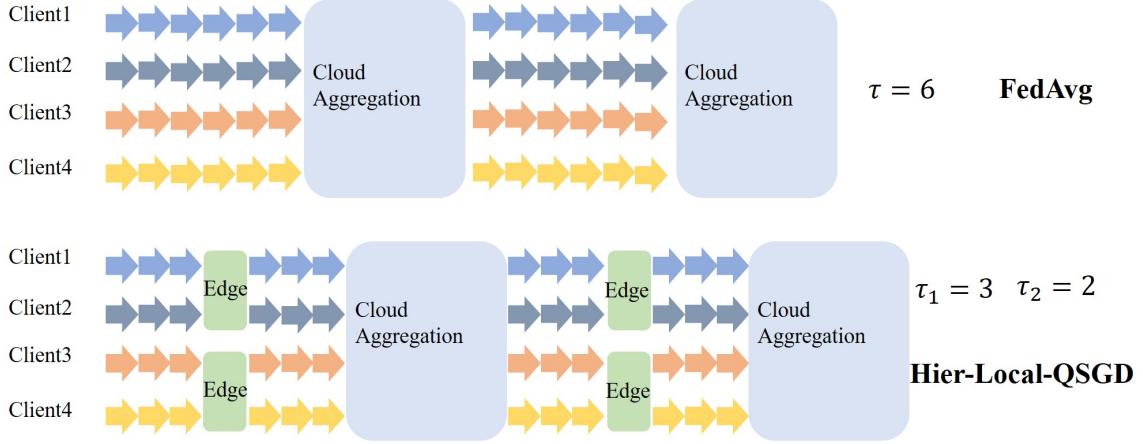


Fig. 2: Comparison of FedAvg and Hier-Local-QSGD.

The evolution of the model parameters x_{k,t_2,t_1}^i , u_{k,t_2}^ℓ and x_k is as follows:

$$\left\{ \begin{array}{l} \text{Local Update: } x_{k,t_2,t_1+1}^i = x_{k,t_2,t_1}^i - \eta \tilde{\nabla} f_i(x_{k,t_2,t_1}^i), \quad 0 \leq t_1 < \tau_1, 0 \leq t_2 < \tau_2 \\ \text{Edge Aggregation: } x_{k,t_2+1,0}^i = u_{k,t_2+1}^\ell = u_{k,t_2}^\ell + \frac{1}{m^\ell} \sum_{i \in C_i^\ell} [Q_1(x_{k,t_2,\tau_1}^i - x_{k,t_2,0}^i)], \quad t_1 = \tau_1, 0 \leq t_2 < \tau_2 \\ \text{Cloud Aggregation: } x_{k+1,0,0}^i = u_{k+1,0}^\ell = x_{k+1} = x_k + \sum_{\ell=1}^S \frac{m^\ell}{n} Q_2(u_{k,\tau_2}^\ell - x_k), \quad t_1 = \tau_1, t_2 = \tau_2 \end{array} \right. \quad (7)$$

IV. CONVERGENCE ANALYSIS

In this section, we present the convergence analysis of the Hier-Local-QSGD algorithm for non-convex loss functions, followed by discussions of the main findings from the obtained convergence bound. We provide a sketch of the proof in this section, while a detailed proof of the key lemmas can be found in the appendix.

A. Challenges in Convergence Analysis

We first highlight the main challenges in the convergence analysis of the proposed algorithm.

- 1) Two levels of aggregation: While the local aggregation at the edge servers can incorporate partial information on the global loss function in a communication-efficient manner, it results in possible gradient divergence at different edge servers, which poses a major challenge in the analysis compared to the *local SGD* algorithm [20], [22].

- 2) Compression of model uploading: The quantization of the local model weights for efficient model uploading will introduce errors in the training process, which has not been analyzed in previous studies for hierarchical FL and requires a delicate analysis.
- 3) Tightness of the upper-bound: There exists an analysis of the hierarchical local SGD for the non-convex loss function, e.g., [13], but the available bound is rather loose. It is highly non-trivial to obtain a tighter bound.

Convergence Criterion: For the error-convergence analysis for non-convex loss functions, the expected gradient norm is often used as an indicator of the convergence [25], [19]. Specifically, an algorithm achieves ϵ -suboptimal if:

$$\mathbb{E} \left[\min_{k=0, \dots, K-1} \|\nabla f(x_k)\|^2 \right] \leq \epsilon.$$

When ϵ is arbitrarily small, the algorithm converges to a first-order stationary point.

B. Additional Notations and Assumptions

To assist the analysis, a virtual auxiliary variable \bar{x}_k is introduced, which is the average of the unquantized updates from the edge servers and defined as follows:

$$\bar{x}_{k+1} = x_k + \sum_{\ell=1}^s \frac{m^\ell}{n} (u_{k, \tau_2}^\ell - u_{k, 0}^\ell). \quad (8)$$

The evolution of the model parameters x_{k, t_2, t_1}^i is specified as follows:

$$x_{k, t_2, t_1}^i = x_k - \eta \sum_{\beta=0}^{t_1-1} \tilde{\nabla} f_i(x_{k, t_2, \beta}^i) - \eta \sum_{\alpha=0}^{t_2-1} \sum_{j \in C^{\ell_i}} \frac{1}{m^{\ell_i}} \mathcal{Q}_1^{(\alpha)} \left[\sum_{\beta=0}^{\tau_1-1} \tilde{\nabla} f_j(x_{k, \alpha, \beta}^j) \right] \quad (9)$$

$$\bar{x}_{k+1} = x_k - \eta \sum_{\ell \in [s]} \frac{m^\ell}{n} \frac{1}{m^\ell} \sum_{\alpha=0}^{\tau_2-1} \sum_{j \in C^\ell} \mathcal{Q}_1^{(\alpha)} \left[\sum_{\beta=0}^{\tau_1-1} \tilde{\nabla} f_j(x_{k, \alpha, \beta}^j) \right] \quad (10)$$

$$x_{k+1} = x_k - \eta \sum_{\ell \in [s]} \frac{m^\ell}{n} \mathcal{Q}_2 \left\{ \frac{1}{m^\ell} \sum_{\alpha=0}^{\tau_2-1} \sum_{j \in C^\ell} \mathcal{Q}_1^{(\alpha)} \left[\sum_{\beta=0}^{\tau_1-1} \tilde{\nabla} f_j(x_{k, \alpha, \beta}^j) \right] \right\} \quad (11)$$

We make standard assumptions on the loss functions and the random quantizer as follows:

Assumption 1 (L-smoothness) The loss function $f(x) : \mathbb{R}^P \rightarrow \mathbb{R}$ is L -smooth with the Lipschitz constant $L > 0$, i.e. :

$$\|\nabla f(x) - \nabla f(y)\| \leq L\|x - y\|$$

for all $x, y \in \mathbb{R}^p$.

Assumption 2 (Variance of SGD) For any fixed model parameter x , the locally estimated stochastic gradient $\tilde{\nabla} f_i(x)$ is unbiased and its variance bounded for any client i , i.e.:

$$\begin{aligned}\mathbb{E}[\tilde{\nabla} f_i(x)|x] &= \nabla f(x), \\ \mathbb{E}[\|\tilde{\nabla} f_i(x) - \nabla f(x)\|^2 |x] &\leq \sigma^2.\end{aligned}$$

Assumption 3 (Unbiased Random Quantizer) The random quantizer $Q(\cdot)$ is unbiased and its variance grows with the squared ℓ_2 norm of its argument, i.e.:

$$\begin{aligned}\mathbb{E}[Q(x)|x] &= x, \\ \mathbb{E}[\|Q(x) - x\|^2 |x] &\leq q \|x\|^2.\end{aligned}$$

C. Main Result and Discussions

The following theorem presents the main convergence result, followed by discussions of key findings.

Theorem 1 (Convergence of Hier-Local-QSGD for non-convex loss functions). Consider a sequence of iterations $\{x_k\}$ at the cloud parameter server generated according to the Hier-Local-QSGD in Algorithm 1. Suppose that the conditions in Assumptions 1, 2, 3 are satisfied, and loss the function f is lower bounded by f^* . Further, define G as:

$$G = 1 - L^2 \eta^2 \left[\frac{\tau_1(\tau_1 - 1)}{2} + \tau_1 \tau_2 \left(\frac{\tau_2(\tau_2 - 1)}{2} + q_1 \tau_2 \right) \right] - L \eta (1 + q_2) \left(\tau_1 \tau_2 + \frac{q_1 \tau_1}{n} \right), \quad (12)$$

where q_1 is the quantization variance parameter for the quantization operator at the client (Q_1 in Algorithm 1), q_2 is the quantization variance parameter for the quantization operator at the edge server (Q_2 in Algorithm 1), and K is the total number of cloud communication rounds. If $G \geq 0$, then the following first-order stationary condition holds:

$$\frac{1}{K} \sum_{k=0}^{K-1} \mathbb{E} \|\nabla f(x_k)\|^2 \leq \frac{2(f(x_0) - f^*)}{\eta K \tau_1 \tau_2} + \frac{L^2 \eta^2}{2} \left[\frac{(1 + q_1)}{n/s} \tau_1(\tau_2 - 1) + (\tau_1 - 1) \right] \sigma^2 + L \eta \frac{1}{n} (1 + q_1)(1 + q_2) \sigma^2. \quad (13)$$

Remark 1 The bound in (13) can be simplified for specific settings. Specifically, letting the step size $\eta = \frac{1}{L\sqrt{T}} = \frac{1}{L\sqrt{K\tau_1\tau_2}}$, we have the following convergence rate:

$$\frac{1}{K} \sum_{k=0}^{K-1} \mathbb{E} \|\nabla f(x_k)\|^2 \leq \frac{2L(f(x_0) - f^*)}{\sqrt{T}} + \frac{1}{T} \frac{1}{2} \left[\frac{(1 + q_1)}{n/s} \tau_1(\tau_2 - 1) + (\tau_1 - 1) \right] \sigma^2 + \frac{1}{\sqrt{T}} \frac{(1 + q_1)(1 + q_2) \sigma^2}{n} \quad (14)$$

Remark 2 When the condition $G \geq 0$ is satisfied, the parameters τ_1, τ_2, q_1, q_2 and η all have a negative influence on the error bound. This means that the optimal parameters to achieve the fastest convergence speed in terms of local update iterations are: $\tau_1 = \tau_2 = 1, q_1 = q_2 = 0$. In this special case, Hier-Local-QSGD degrades to the conventional SGD. Note that this does not mean that the convergence will be the fastest in the wall clock time, as the communication latency is different for the edge side update and the cloud side update.

Remark 3 When $\tau_2 = 1, q_1 = q_2 = 0$, which means that there is no partial aggregation nor quantization, we recover the result of [22]. One thing to notice is that our result does not coincide exactly with the result in [6] for the two-layer *FedPAQ* algorithm when we set $\tau_2 = 1$, i.e., FedAvg with quantization. This is because the expected gradient norm on the left hand side of (13) is different. An average of the expected gradient norm for the model parameters after every $\tau_1\tau_2$ updates, i.e. $\{x_k\}_{k=0,\dots,K-1}$, is considered in this paper, while an average of the expected gradient norm for the auxiliary virtual model parameters at every update step, i.e., $\{\bar{x}_{k,t}\}_{k=0,\dots,K-1,t=0,\dots,\tau}$, is considered in [6].

Remark 4 For the locally estimated gradient $\tilde{\nabla}f$, a batch of data of size b can also be used, where the only difference in the analysis will be that of the variance of the SGD in Assumption 2 decreases from σ^2 to σ^2/b .

Remark 5 One implication of the bound is that the fewer the number of edge servers, i.e., s , the faster the convergence. When the number of participated clients in an FL system is fixed, the partial edge aggregation will incorporate more clients if there are fewer edge servers available in the system. The variance caused by the partial aggregation decreases, and hence the convergence will be faster.

Remark 6 In our result, we show that the error bound caused by the multiple steps of local updates is linear to the aggregation interval, i.e. $\tau_1\tau_2$. In [13], convergence analysis for non-convex functions has also been provided and their error bound is quadratic. Thus, their bound is looser than ours.

Remark 7 The distribution of the clients under the edge, i.e. $\{m^\ell\}_{\ell=1,\dots,s}$ has no influence on the convergence, which is quite counter intuitive. This conclusion can help us decouple the learning performance and edge-client association for performance optimization in hierarchical FL, which will be further elaborated in Section V.

D. Proof Outline

We now give an outline of the proof for Theorem 1. Detailed proofs of the lemmas are deferred to Appendix A.

The proof proceeds as follows: using the property of L -smooth functions, we first prove a bound in Lemma 1 of the evolution process of the cloud model parameter $\{x_k\}$, which depends on three terms, i.e. $\mathbb{E} \langle \nabla f(x_k), \bar{x}_{k+1} - x_k \rangle$, $\mathbb{E} \|\bar{x}_{k+1} - x_k\|^2$, and $\mathbb{E} \|x_{k+1} - \bar{x}_{k+1}\|^2$. In Lemmas 2, 3, 4, we then derive upper bounds of the three terms respectively, and characterize their relationships to the aggregation parameters τ_1, τ_2 and the quantization variance parameters q_1, q_2 .

Lemma 1 (One round of global aggregation) With Assumptions 1 and 2, we have the following relationship between x_{k+1} and x_k :

$$\mathbb{E}f(x_{k+1}) - \mathbb{E}f(x_k) \leq \mathbb{E} \langle \nabla f(x_k), \bar{x}_{k+1} - x_k \rangle + \frac{L}{2} \mathbb{E} \|\bar{x}_{k+1} - x_k\|^2 + \frac{L}{2} \mathbb{E} \|x_{k+1} - \bar{x}_{k+1}\|^2 \quad (15)$$

Lemma 1 follows from the property of the L -smoothness in Assumption 1, we next bound the three terms on the right hand side of Eqn. (15) respectively.

Lemma 2 With Assumptions 1, 2 and 3, $\mathbb{E} \langle \nabla f(x_k), \bar{x}_{k+1} - x_k \rangle$ is bounded as follows:

$$\begin{aligned} & \mathbb{E} \langle \nabla f(x_k), \bar{x}_{k+1} - x_k \rangle \\ & \leq -\frac{\eta}{2} \left\{ 1 - L^2 \eta^2 \left[\frac{\tau_1(\tau_1 - 1)}{2} + \tau_1 \tau_2 \left(\frac{\tau_2(\tau_2 - 1)}{2} + q_1 \tau_2 \right) \right] \right\} \frac{1}{n} \sum_{i=1}^n \sum_{\alpha=0}^{\tau_2-1} \sum_{\beta=0}^{\tau_1-1} \mathbb{E} \left\| \nabla f(x_{k,\alpha,\beta}^i) \right\|^2 \\ & \quad + \frac{\tau_1 \tau_2}{2} \left[(\tau_1 - 1) + \frac{S}{n} (1 + q_1) \tau_1 (\tau_2 - 1) \right] \sigma^2 \end{aligned}$$

Lemma 3 With Assumptions 1, 2 and 3, then $\mathbb{E} \|\bar{x}_{k+1} - x_k\|^2$ is bounded as follows:

$$\mathbb{E} \|\bar{x}_{k+1} - x_k\|^2 \leq \eta^2 \left(\tau_1 \tau_2 + \frac{q_1 \tau_1}{n} \right) \frac{1}{n} \sum_{i=1}^n \sum_{\alpha=0}^{\tau_2-1} \sum_{\beta=0}^{\tau_1-1} \mathbb{E} \left\| \nabla f(x_{k,\alpha,\beta}^i) \right\|^2 + \eta^2 \frac{1}{n} (1 + q_1) \tau_1 \tau_2 \sigma^2 \quad (16)$$

Lemma 4 With Assumptions 1, 2 and 3, then $E \|x_{k+1} - \bar{x}_{k+1}\|^2$ is bounded as follows:

$$E \|x_{k+1} - \bar{x}_{k+1}\|^2 \leq \eta^2 q_2 \left(\tau_1 \tau_2 + \frac{q_1 \tau_1}{n} \right) \frac{1}{n} \sum_{i=1}^n \sum_{\alpha=0}^{\tau_2-1} \sum_{\beta=0}^{\tau_1-1} \mathbb{E} \left\| \nabla f(x_{k,\alpha,\beta}^i) \right\|^2 + \eta^2 \frac{1}{n} (1 + q_1) q_2 \tau_1 \tau_2 \sigma^2 \quad (17)$$

By combining Lemmas 1 to 4, we now have the following:

$$\mathbb{E}f(x_{k+1}) - \mathbb{E}f(x_k) \leq -\frac{\eta}{2} \tau_1 \tau_2 \mathbb{E} \|\nabla f(x_k)\|^2 \quad (18)$$

$$\begin{aligned}
& -\frac{\eta}{2} \left\{ 1 - L^2 \eta^2 \left[\frac{\tau_1(\tau_1 - 1)}{2} + \tau_1 \tau_2 \left(\frac{\tau_2(\tau_2 - 1)}{2} + q_1 \tau_2 \right) \right] - L\eta(1 + q_2) \left(\tau_1 \tau_2 + \frac{q_1 \tau_1}{n} \right) \right\} \frac{1}{n} \sum_{i=1}^n \sum_{\alpha=0}^{\tau_2-1} \sum_{\beta=0}^{\tau_1-1} \mathbb{E} \left\| \nabla f(x_{k,\alpha,\beta}^i) \right\|^2 \\
& + \frac{L^2 \eta^3}{4} \tau_1 \tau_2 \left[(\tau_1 - 1) + \frac{s}{n} (1 + q_1) \tau_1 (\tau_2 - 1) \right] \sigma^2 + \frac{L\eta^2}{2} \frac{1}{n} (1 + q_1)(1 + q_2) \tau_1 \tau_2 \sigma^2
\end{aligned} \tag{19}$$

For a sufficiently small η , when the following condition is satisfied:

$$1 - L^2 \eta^2 \left[\frac{\tau_1(\tau_1 - 1)}{2} + \tau_1 \tau_2 \left(\frac{\tau_2(\tau_2 - 1)}{2} + q_1 \tau_2 \right) \right] - L\eta(1 + q_2) \left(\tau_1 \tau_2 + \frac{q_1 \tau_1}{n} \right) \geq 0. \tag{20}$$

we have:

$$\begin{aligned}
\mathbb{E}f(x_{k+1}) - \mathbb{E}f(x_k) & \leq -\frac{\eta}{2} \tau_1 \tau_2 \mathbb{E} \left\| \nabla f(x_k) \right\|^2 \\
& + \frac{L^2 \eta^3}{4} \tau_1 \tau_2 \left[(\tau_1 - 1) + \frac{s}{n} (1 + q_1) \tau_1 (\tau_2 - 1) \right] \sigma^2 + \frac{L\eta^2}{2} \frac{1}{n} (1 + q_1)(1 + q_2) \tau_1 \tau_2 \sigma^2
\end{aligned} \tag{21}$$

By summing (21) over the $k = 0, \dots, K - 1$ and re-arranging the terms, we obtain the main result in Theorem 1.

Now, we have derived the convergence result for the proposed Hier-Local-QSGD algorithm w.r.t. the update iterations, i.e., k . Next, by applying the theoretical analysis to two design problems, we illustrate how it can be used to improve the communication efficiency of the hierarchical FL system.

V. APPLICATIONS OF CONVERGENCE ANALYSIS

In this section, we illustrate the utility of the convergence analysis by investigating two key design problems in hierarchical FL, i.e., the accuracy-latency trade-off and the edge-client association.

A. Accuracy-latency Trade-off

The proposed Hier-Local-QSGD training algorithm improves the communication efficiency by allowing partial edge aggregation and quantization on the model updates. Compared with the FedAvg algorithm for cloud-based FL, Hier-Local-QSGD leverages efficient low-latency edge aggregation to reduce the propagation latency, which, however, introduces additional variance in the training process. Specifically, compressing the model to be uploaded reduces the propagation latency by reducing the message size, but the distortion of the quantization also introduces

additional variance in the training process. Thus, to train a good model within a given deadline, the parameters τ_1, τ_2, q_1, q_2 need to be properly designed.

To illustrate the trade-off between the learning performance and then the communication efficiency, we adopt the communication model of [8] with homogeneous clients. Consider the case where for all the clients, the local computation time for one SGD iteration is D_{comp} , the communication delay of transmitting a full-precision model updates between the client (device) and edge is D_{de} , and the communication delay of transmitting a full-precision model between the edge and cloud is D_{ec} . For the quantizer, we use the random sparsification operator in Example 1, which is unbiased and its quantization variance parameter q grows as the number of non-zero elements in the mask, i.e., r , decreases. Specifically, for a d -dimensional vector, it can be shown that $q = \frac{d}{r} - 1$. Encoding the indices of the random r elements can be done with additional $O(r \log(d))$ bits [27]. We assume that the unquantized d -dimensional vector needs $32d$ bits to represent. Thus, the communication delay for transmitting a compressed update is:

$$D^q = \frac{32 + \log(d)}{32(1 + q)} D, \quad (22)$$

where q is the variance parameter of the random sparsification operator, and D is the latency for transmitting the unquantized updates. Then, after K rounds of cloud-aggregation in total, the training latency T is:

$$T = K \left(\tau_1 \tau_2 D_{comp} + \tau_2 D_{de} \frac{32 + \log(d)}{32(1 + q_1)} + D_{ec} \frac{32 + \log(d)}{32(1 + q_2)} \right) \quad (23)$$

By substituting (23) into (26), the minimal expected gradient squared gradient norm within T time is bounded by:

$$\frac{2(f(x_0) - f^*)}{T} \left(D_{comp} + \frac{D_{de} \frac{32 + \log(d)}{32(1 + q_1)}}{\tau_1} + \frac{D_{ec} \frac{32 + \log(d)}{32(1 + q_2)}}{\tau_1 \tau_2} \right) + \frac{L^2 \eta^2}{2} \left[\frac{(1 + q_1)}{n/s} \tau_1 (\tau_2 - 1) + (\tau_1 - 1) \right] \sigma^2 + L \eta \frac{1}{n} (1 + q_1)(1 + q_2) \sigma^2 \quad (24)$$

From the bound in (24), we can clearly see the accuracy-latency trade-off when choosing different τ_1, τ_2, q_1, q_2 . Specifically, when we choose larger values for τ_1, τ_2, q_1, q_2 , the infrequent communication and low-precision quantization reduces the transmission latency and decreases the first term in (24). Meanwhile, an additional noise is introduced into the training process and hence increases the last two terms in (24). For a given setting and specific performance requirement, e.g., a deadline of training, we can determine the values of these key parameters accordingly through minimizing (24) by setting the derivatives w.r.t. corresponding parameters

to zero. We will empirically demonstrate this trade-off in the simulations in Section VI.

B. Edge-client Association

Edge-client association is a unique resource allocation problem in Hierarchical Federated Edge Learning. This problem has also been discussed in [15] with a different convergence analysis framework to capture the learning performance jointly with resource allocation to accelerate training and save energy. Intuitively, it will be beneficial to the overall learning performance to have a large number of devices connected to each edge server. However, for a given edge server with limited spectrum resources, when more clients, i.e., mobile devices, are connected to the server, less bandwidth will be assigned to each client, which results in a longer communication delay. Thus, the learning performance and spectrum resource allocation are intertwined with each other, which makes the optimization problem different from the general computation offloading problem in the conventional MEC framework [28].

In this paper, by analyzing the convergence of the Hierarchical Federated Learning with the Hier-Local-QSGD algorithm, we find that, under the IID-data distribution, when the number of edge servers is fixed and each edge server is associated with at least one client, the convergence speed w.r.t to the iterations is irrelevant to the client-edge association strategy, as discussed in Remark 7. Thus, to accelerate training of the overall system, we only need to minimize the communication delay for each aggregation. Due to the synchronization requirement in the Hier-Local-QSGD training algorithm at each aggregation step, the delay for each aggregation step is determined by the slowest client.

We notice that a recent work [14] also analyzed the hierarchical local SGD algorithm for general non-convex loss functions with non-IID data. In their convergence result, the client-distribution will influence the final error bound, in contrast to what we observed in Remark 7. For the convenience of comparison and explanation, we present their training algorithm and the proved convergence result under the IID data distribution as follows using the notations in this paper:

Model parameter evolution with the training algorithm in [14], HF-SGD:

$$\left\{ \begin{array}{l} \text{Local Update: } x_{k,t_2,t_1+1}^i = x_{k,t_2,t_1}^i - \eta \tilde{\nabla} f_i(x_{k,t_2,t_1}^i), \quad 0 \leq t_1 < \tau_1, 0 \leq t_2 < \tau_2 \\ \text{Edge Aggregation: } x_{k,t_2+1,0}^i = u_{k,t_2+1}^\ell = u_{k,t_2}^\ell + \frac{1}{m^\ell} \sum_{i \in C_i^\ell} (x_{k,t_2,\tau_1}^i - x_{k,t_2,0}^i), \quad t_1 = \tau_1, 0 \leq t_2 < \tau_2 \\ \text{Cloud Aggregation: } x_{k+1,0,0}^i = u_{k+1,0}^\ell = x_{k+1} = x_k + \sum_{\ell=1}^s \frac{1}{s} (u_{k,\tau_2}^\ell - x_k), \quad t_1 = \tau_1, t_2 = \tau_2 \end{array} \right. \quad (25)$$

Consider an auxiliary variable:

$$\bar{x}^t = \frac{1}{n} \sum_{i=1}^n x_{k,t_2,t_1}^i, \quad t = k\tau_1\tau_2 + t_2\tau_2 + t_1$$

The convergence analysis in [14] is stated as follows:

Theorem 2 (Corollary 1 in [14] with IID data). Consider the problem in (5), and apply the HF-SGD training algorithm. Assuming Assumptions 1 to 3 are satisfied, and choosing the step size $\eta < \frac{1}{2\sqrt{6}L\tau_1\tau_2}$, then for any $T > 1$, we have:

$$\begin{aligned} & \frac{1}{T} \sum_{t=0}^{T-1} \mathbb{E} \|\nabla f(\bar{x}_t)\| \\ & \leq \frac{2(f(x_0) - f^*)}{\eta T} + \eta L \sigma^2 \frac{1}{s^2} \sum_{\ell=1}^s \frac{1}{m^\ell} + 2C\eta^2 \tau_1 \tau_2 L^2 \left(1 - \frac{1}{s}\right) \left(\sigma^2 \frac{1}{s} \sum_{\ell=1}^s \frac{1}{m^\ell}\right) \\ & \quad + \frac{2C\eta^2 L^2 \sigma^2}{s} \sum_{\ell=1}^s \left(1 - \frac{1}{m^\ell}\right) \tau_1 \end{aligned} \quad (26)$$

where $C = 40/3$.

From Eqn. (26), we see that the client-edge distribution $\{m^\ell\}_{\ell=1,\dots,s}$ has an impact on the error bound, which is different from our result. We notice that this is because different weight coefficients are used when averaging the updates from the edge to the cloud. In our Hier-Local-QSGD algorithm, the weighted coefficient m^ℓ/n is used while in the HF-SGD algorithm in [14], the uniform coefficient $1/s$ is used. When performing partial edge aggregation, the additional variance introduced by partial aggregation is inversely proportional to the number of clients to be aggregated, i.e., m^ℓ . Thus, adopting a weighted average policy at the cloud aggregation step will balance the additional variance that is introduced by the edge server with fewer clients while a uniform average policy fails to do so.

TABLE II: The latency parameters for the communication and computation of a full-precision model *MNIST* and *CIFAR-10*.

Dataset	T^{comp}	T^{comm}
<i>MNIST</i>	0.005s	0.1233s
<i>CIFAR-10</i>	0.8s	33s

VI. NUMERICAL RESULTS

In this section, we present sample simulation results for Hier-Local-QSGD to verify the observations from the convergence analysis and illustrate the advantages of the hierarchical FL system. As the advantage over the edge-based FL system in terms of the model accuracy is evidently shown in Fig. 1b. We shall focus on the comparison with the cloud-based FL system, which is equivalent to the case with $\tau_2 = 1$ in our Hier-Local-QSGD algorithm.

A. Settings

We consider a hierarchical FL system with n clients, s edge servers and a cloud server, assuming that edge server ℓ authorizes m^ℓ clients, each with the same amount of IID training data. We consider an image classification task on standard datasets *MNIST* [17] and *CIFAR-10* [18]. For the 10-class hand-written digit classification dataset *MNIST*, we use the Convolutional Neural Network (CNN) with 21840 trainable parameters as in [3]. For the local computation of the training with *MNIST* on each client, we employ mini-batch Stochastic Gradient Descent (SGD) with batch size 4, and an initial learning rate of 0.01 which decays exponentially at a rate of 0.995 with every epoch. For the *CIFAR-10* dataset, we use a CNN with 3 convolutional blocks, which has 5852170 parameters and achieves 90% testing accuracy in centralized training. For the local computation of the training with *CIFAR-10*, mini-batch SGD is also employed with a batch size of 4, an initial learning rate of 0.1 and an exponential learning rate decay of 0.992 for every epoch.

The modeling of the computing and communication latency during the training process largely follows [7]. We assume homogeneous communication conditions and computing resources for different clients. For the communication channel between the client and edge server, clients upload the model through a wireless channel of 1 MHz bandwidth with a channel gain g equals to 10^{-8} . The transmitter power p is fixed at 0.5W, and the noise power σ is 10^{-10} W. For the local computation model, the number of CPU cycles to execute one sample c is assumed to be

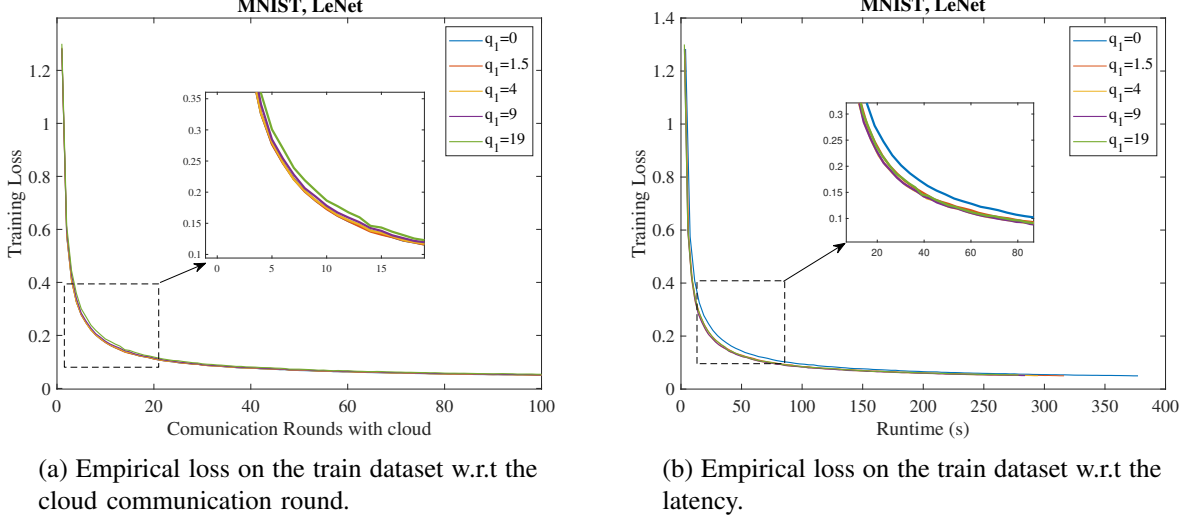


Fig. 3: Accuracy-latency trade-off w.r.t. q_1 , MNIST, $\tau_1 = 50$, $\tau_2 = 6$, $q_2 = 0$.

20 cycles/bit, the CPU cycle frequency f is 1 GHz and the effective capacitance is 2×10^{-28} . For the communication latency to the cloud, we assume it is 10 times larger than that to the edge. Assume the uploaded model size is W bits, and one local iteration involves D bits of data. In this case, the latency and energy consumption for one full-precision model upload and one local iteration can be calculated with the following equations (specific parameters are shown in Table II):

$$T^{comp} = \frac{cD}{f}, \quad T^{comm} = \frac{W}{B \log_2(1 + \frac{hp}{\sigma})} \quad (27)$$

B. Accuracy-latency Trade-off

We investigate the accuracy-latency trade-off introduced by the quantization scheme and the partial edge aggregation separately. Fig. 3 shows the influence of the quantization operator, for the MNIST dataset with the aggregation interval of $\tau_1 = 50$, $\tau_2 = 6$, the quantization parameter $q_1 = 9$ attains the fastest convergence w.r.t. latency. In Fig. 4 with the CIFAR-10 dataset, by varying the choice of aggregation interval, τ_1, τ_2 , we see that a smaller τ_1 achieves a fastest convergence speed w.r.t. the iterations, i.e., the cloud communication rounds. But in terms of latency, $\tau_1 = 50$, $\tau_2 = 5$ and $\tau_1 = 25$, $\tau_2 = 10$ achieve better performance.

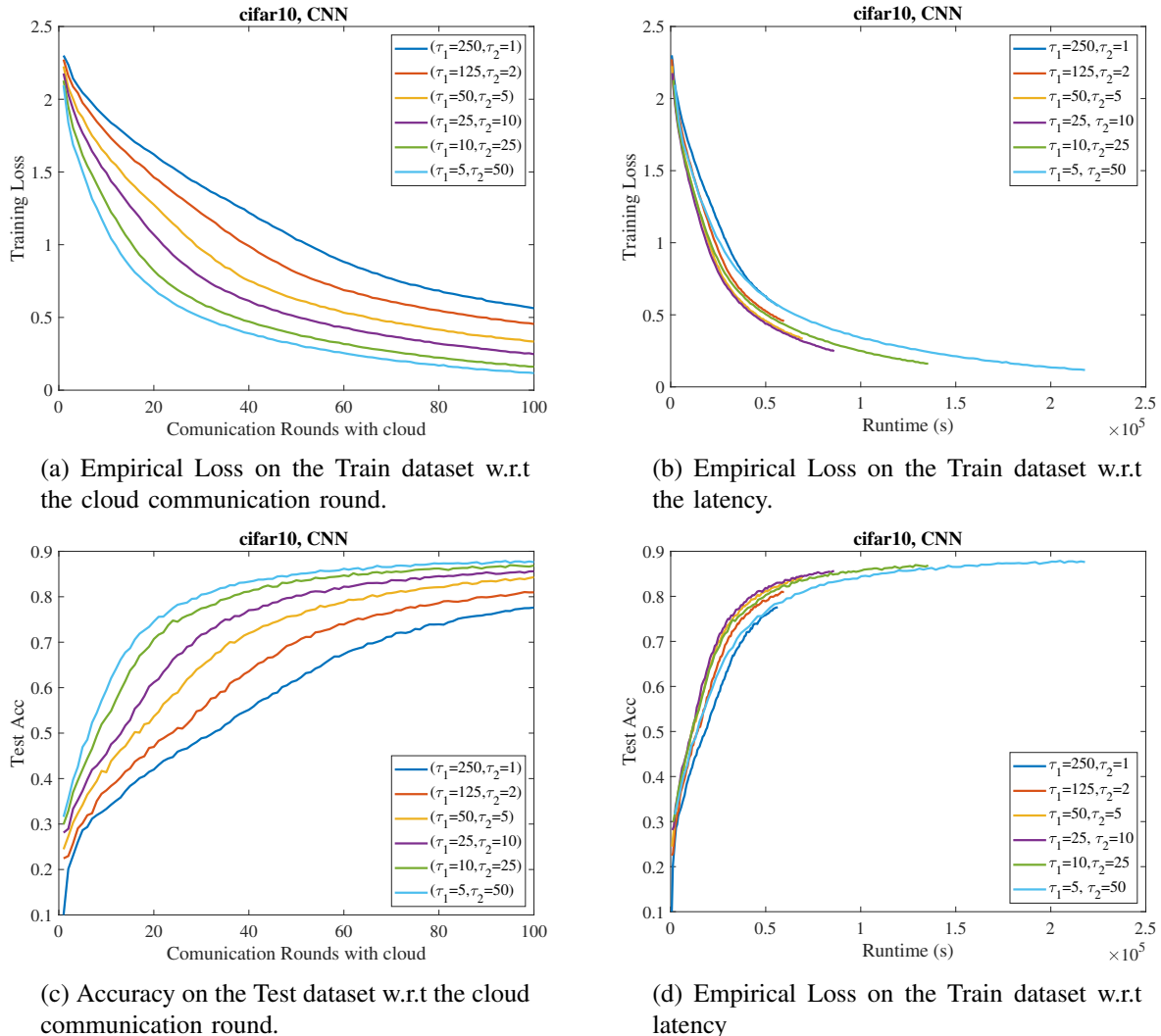
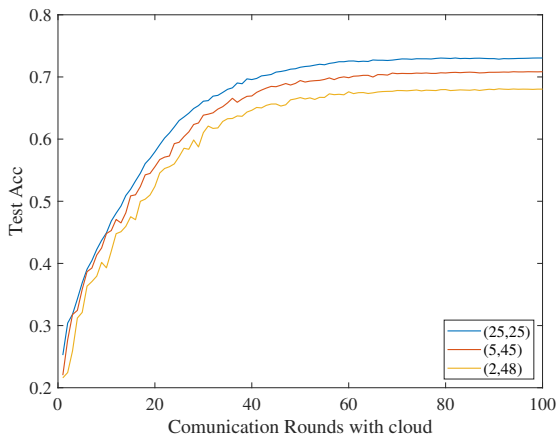


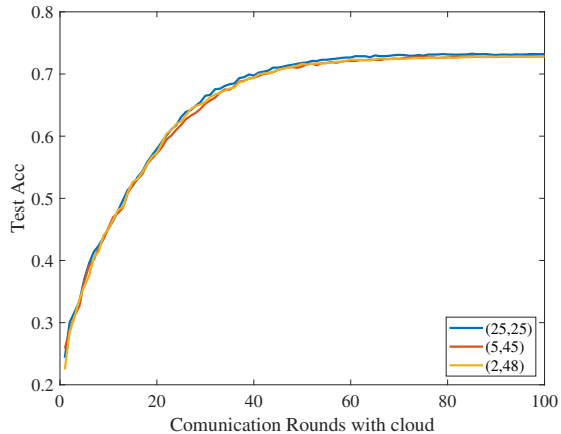
Fig. 4: Accuracy-latency trade-off w.r.t. τ_1, τ_2 , CIFAR-10, $q_1 = q_2 = 0$.

C. Edge-client Association

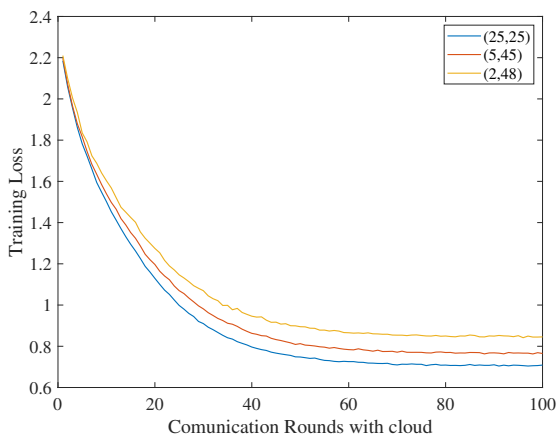
In this part, we show that when using our training algorithm Hier-Local-QSGD, the learning performance is irrelevant to the edge-client association strategy. As revealed in our analysis in Section V, this is because at each aggregation step, the weighted average scheme can balance the variance. As shown in Fig. 5, we consider a hierarchical system with 50 clients, 2 edge servers with three different client-edge association cases, i.e., (25, 25), (45, 5), (48, 2), denoting the numbers of clients associated with the two edge servers. It is seen from Fig. 5 that for Hier-Local-QSGD which adopts the weighted average scheme, the two learning curves, i.e., the testing accuracy and the training loss, coincide with each other. While for the uniform average,



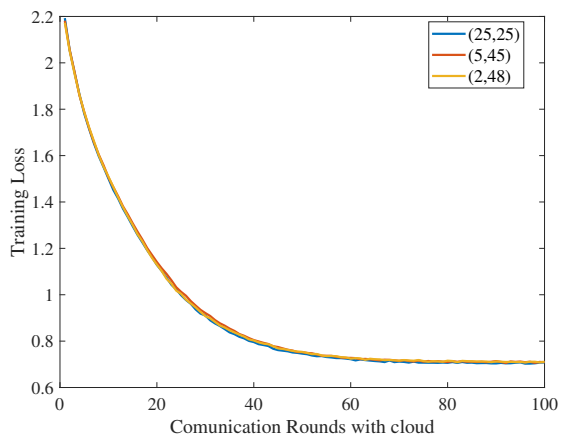
(a) Accuracy on the test dataset w.r.t the cloud communication round, uniform average [15].



(b) Accuracy on the test dataset w.r.t the cloud communication round, Hier-Local-QSGD with weighted average.



(c) Empirical loss on the train dataset w.r.t the cloud communication round, uniform average [15].



(d) Empirical loss on the train dataset w.r.t the cloud communication round, Hier-Local-QSGD with weighted average.

Fig. 5: Performance with different edge-client association strategies, CIFAR-10, $\tau_1 = 50, \tau_2 = 5, q_2 = q_1 = 0, n = 50, s = 2$

the learning curves diverge and (25, 25) is the best one, since in this case uniform averaging is the same with weighted averaging.

VII. CONCLUSIONS

This paper investigated Hierarchical Quantized Federated Learning, which naturally leverages the client-edge-cloud network hierarchy and quantized model updates to improve the communication efficiency of the training process of FL. We provided a tight convergence bound for the Hier-Local-QSGD training algorithm with non-convex loss functions. The utility of such analysis

was illustrated in two design problems in hierarchical FL. We further provided empirical results to evaluate the performance of Hier-Local-QSGD and verify the observations from the analysis, as well as, demonstrate the trade-off between accuracy and latency in hierarchical FL.

One limitation of the current analysis is that it focused on the IID-data, which leads to the conclusion that the edge-client association has no influence on the convergence speed. It would be interesting to extend the analysis of Hier-Local-QSGD to the non-IID case and further investigate the edge-client problem. Finally, it is noted that we demonstrated the accuracy-latency trade-off in the hierarchical FL system. Designing an adaptive communication strategy that determines the parameters, i.e., τ_1, τ_2, q_1, q_2 during the training process is an interesting problem of practical importance and requires further investigation.

APPENDIX

Proofs of Key Lemmas

Proof. Lemma 1: The proof directly follows from the property of the L -smoothness:

$$f(x) \leq f(y) + \langle \nabla f(y), x - y \rangle + \frac{L}{2} \|x - y\|^2. \quad (28)$$

for any L -smooth function f and variables x, y . Then under the L -smooth assumption:

$$f(x_{k+1}) \leq f(\bar{x}_{k+1}) + \langle \nabla f(\bar{x}_{k+1}), x_{k+1} - \bar{x}_{k+1} \rangle + \frac{L}{2} \|x_{k+1} - \bar{x}_{k+1}\|^2. \quad (29)$$

$$f(\bar{x}_{k+1}) \leq f(x_k) + \langle \nabla f(x_k), \bar{x}_{k+1} - x_k \rangle + \frac{L}{2} \|\bar{x}_{k+1} - x_k\|^2. \quad (30)$$

By taking expectations of both sides of (29) and from Eqns. (10), (11) and the unbiased assumption of the random quantizer Q_2 , we have $\mathbb{E}_{Q_2}[x_{k+1}] = \bar{x}_{k+1}$, so that (29) becomes:

$$\mathbb{E}f(x_{k+1}) \leq \mathbb{E}f(\bar{x}_{k+1}) + \frac{L}{2} \mathbb{E} \|x_{k+1} - \bar{x}_{k+1}\|^2 \quad (31)$$

Similarly, by taking expectation over (30) and combining it with (31), Lemma 1 is proved. \square

Proof. Lemma 2: From Eqn. (10), we have:

$$\bar{x}_{k+1} - x_k = -\eta \sum_{\ell \in [s]} \frac{m^\ell}{n} \frac{1}{m^\ell} \sum_{\alpha=0}^{\tau_2-1} \sum_{j \in C^\ell} Q_1^{(\alpha)} \left[\sum_{\beta=0}^{\tau_1-1} \tilde{\nabla} f_j(x_{k, \alpha, \beta}^j) \right] \quad (32)$$

Then by taking the expectation and changing the subscript from (α, β) to (t_2, t_1) , we obtain:

$$\mathbb{E} \langle \nabla f(x_k), \bar{x}_{k+1} - x_k \rangle = -\mathbb{E} \langle \nabla f(x_k), \eta \sum_{\ell \in [s]} \frac{m^\ell}{n} \frac{1}{m^\ell} \sum_{\alpha=0}^{\tau_2-1} \sum_{j \in C^\ell} Q_1^{(\alpha)} \left[\sum_{\beta=0}^{\tau_1-1} \tilde{\nabla} f_j(x_{k, \alpha, \beta}^j) \right] \rangle \quad (33)$$

$$= -\eta \sum_{j \in [n]} \frac{1}{n} \sum_{t_2=0}^{\tau_2-1} \sum_{t_1=0}^{\tau_1-1} \mathbb{E}_{\{Q_1^{(\alpha)}, \{\xi_{k, \alpha, \beta}^j\}_{\beta=0}^{\tau_1-1}\}_{\alpha=0}^{\tau_2-1}, \{\xi_{k, t_2, \beta}^j\}_{\beta=0}^{t_1-1}} \langle \nabla f(x_k), \nabla f(x_{k, t_2, t_1}^j) \rangle \quad (34)$$

Here for each tuple of (k, t_2, t_1) , \mathbb{E} means taking expectation of the randomness generated from the SGD and random quantization scheme happened before step (k, t_2, t_1) .

For the simplicity of notation, we omit the subscript of the expectation operation and use \mathbb{E} . Using the identity : $2\langle \mathbf{a}, \mathbf{b} \rangle = \|\mathbf{a}\|^2 + \|\mathbf{b}\|^2 - \|\mathbf{a} - \mathbf{b}\|^2$, we have:

$$-\mathbb{E} \langle \nabla f(x_k), \nabla f(x_{k, t_2, t_1}^j) \rangle = -\frac{1}{2} \mathbb{E} \|\nabla f(x_k)\|^2 - \frac{1}{2} \mathbb{E} \|\nabla f(x_{k, t_2, t_1}^j)\|^2 + \frac{1}{2} \mathbb{E} \|\nabla f(x_k) - \nabla f(x_{k, t_2, t_1}^j)\|^2 \quad (35)$$

Now, we will bound the third term on the RHS of (35).

$$\mathbb{E} \left\| \nabla f(x_k) - \nabla f(x_{k,t_2,t_1}^j) \right\|^2 = L^2 \eta^2 \mathbb{E} \left\| \sum_{\beta=0}^{t_1-1} \tilde{\nabla} f_i(x_{k,t_2,\beta}^i) + \sum_{\alpha=0}^{t_2-1} \sum_{j \in C^{\ell_i}} \frac{1}{m^{\ell_i}} Q_1^{(\alpha)} \left[\sum_{\beta=0}^{\tau_1-1} \tilde{\nabla} f_j(x_{k,\alpha,\beta}^j) \right] \right\|^2 \quad (36)$$

Then using $\mathbb{E}\|x\|^2 = \|\mathbb{E}x\|^2 + \text{Var}(x)^2$:

$$\mathbb{E} \left\| \sum_{\beta=0}^{t_1-1} \tilde{\nabla} f_i(x_{k,t_2,\beta}^i) + \sum_{\alpha=0}^{t_2-1} \sum_{j \in C^{\ell_i}} \frac{1}{m^{\ell_i}} Q_1^{(\alpha)} \left[\sum_{\beta=0}^{\tau_1-1} \tilde{\nabla} f_j(x_{k,\alpha,\beta}^j) \right] \right\|^2 \quad (37)$$

$$= \mathbb{E} \underbrace{\left\| \sum_{\beta=0}^{t_1-1} \nabla f(x_{k,t_2,\beta}^i) + \sum_{\alpha=0}^{t_2-1} \sum_{j \in C^{\ell_i}} \frac{1}{m^{\ell_i}} \left[\sum_{\beta=0}^{\tau_1-1} \nabla f(x_{k,\alpha,\beta}^j) \right] \right\|^2}_A \quad (38)$$

$$+ \mathbb{E} \underbrace{\left\| \sum_{\beta=0}^{t_1-1} \left[\tilde{\nabla} f_i(x_{k,t_2,\beta}^i) - \nabla f(x_{k,t_2,\beta}^i) \right] + \sum_{\alpha=0}^{t_2-1} \sum_{j \in C^{\ell_i}} \frac{1}{m^{\ell_i}} \left\{ Q_1^{(\alpha)} \left[\sum_{\beta=0}^{\tau_1-1} \tilde{\nabla} f_j(x_{k,\alpha,\beta}^j) \right] - \sum_{\beta=0}^{\tau_1-1} \nabla f(x_{k,\alpha,\beta}^j) \right\} \right\|^2}_B \quad (39)$$

$$= \mathbb{E} \underbrace{\left\| \sum_{\beta=0}^{t_1-1} \nabla f(x_{k,t_2,\beta}^i) + \sum_{\alpha=0}^{t_2-1} \sum_{j \in C^{\ell_i}} \frac{1}{m^{\ell_i}} \left[\sum_{\beta=0}^{\tau_1-1} \nabla f(x_{k,\alpha,\beta}^j) \right] \right\|^2}_A \quad (40)$$

$$+ \underbrace{\sum_{\beta=0}^{t_1-1} \mathbb{E} \left\| \tilde{\nabla} f_i(x_{k,t_2,\beta}^i) - \nabla f(x_{k,t_2,\beta}^i) \right\|^2}_{B_1} + \underbrace{\sum_{\alpha=0}^{t_2-1} \mathbb{E} \left\| \sum_{j \in C^{\ell_i}} \frac{1}{m^{\ell_i}} \left\{ Q_1^{(\alpha)} \left[\sum_{\beta=0}^{\tau_1-1} \tilde{\nabla} f_j(x_{k,\alpha,\beta}^j) \right] - \sum_{\beta=0}^{\tau_1-1} \nabla f(x_{k,\alpha,\beta}^j) \right\} \right\|^2}_{B_2} \quad (41)$$

The inner product vanished when B is expanded, and the conditional independence is used:

$$1) \mathbb{E} \left\langle \nabla f(x_{k,t_2,s}^j) - \tilde{\nabla} f_j(x_{k,t_2,s}^j), \nabla f(x_{k,t_2,s}^j) - \tilde{\nabla} f_j(x_{k,t_2,s}^j) \right\rangle, \forall s < t$$

$$\begin{aligned} & \mathbb{E}_{x_{k,t_2,s}^j, \xi_{k,t_2,s}^j, x_{k,t_2,t}^j, \xi_{k,t_2,t}^j} \left\langle \nabla f(x_{k,t_2,s}^j) - \tilde{\nabla} f_j(x_{k,t_2,s}^j), \nabla f(x_{k,t_2,s}^j) - \tilde{\nabla} f_j(x_{k,t_2,s}^j) \right\rangle \\ &= \mathbb{E}_{x_{k,t_2,s}^j, \xi_{k,t_2,s}^j, x_{k,t_2,t}^j} \left\langle \nabla f(x_{k,t_2,s}^j) - \tilde{\nabla} f_j(x_{k,t_2,s}^j), \mathbb{E}_{\xi_{k,t_2,t}^j} \left[\nabla f(x_{k,t_2,s}^j) - \tilde{\nabla} f_j(x_{k,t_2,s}^j) \right] \right\rangle = 0 \end{aligned}$$

$$2) \mathbb{E} \left\langle \nabla f(x_{k,t_2,s}^j) - \tilde{\nabla} f_j(x_{k,t_2,s}^j), \sum_{j \in C^{\ell_i}} \left\{ Q_1^{(\alpha)} \left[\sum_{\beta=0}^{\tau_1-1} \tilde{\nabla} f_j(x_{k,\alpha,\beta}^j) \right] - \sum_{\beta=0}^{\tau_1-1} \nabla f(x_{k,\alpha,\beta}^j) \right\} \right\rangle:$$

$$\begin{aligned} & \mathbb{E}_{x_{k,t_2,s}^j, \xi_{k,t_2,s}^j, \{x_{k,\alpha,\beta}^j\}_{\beta=0}^{\tau_1}, \{\xi_{k,\alpha,\beta}^j\}_{\beta=0}^{\tau_1}} \left\langle \nabla f(x_{k,t_2,s}^j) - \tilde{\nabla} f_j(x_{k,t_2,s}^j), \sum_{j \in C^{\ell_i}} \left\{ Q_1^{(\alpha)} \left[\sum_{\beta=0}^{\tau_1-1} \tilde{\nabla} f_j(x_{k,\alpha,\beta}^j) \right] - \sum_{\beta=0}^{\tau_1-1} \nabla f(x_{k,\alpha,\beta}^j) \right\} \right\rangle \\ &= \mathbb{E}_{x_{k,t_2,s}^j, \{x_{k,\alpha,\beta}^j\}_{\beta=0}^{\tau_1}, \{\xi_{k,\alpha,\beta}^j\}_{\beta=0}^{\tau_1}} \left\langle \mathbb{E}_{\xi_{k,t_2,s}^j} \left[\nabla f(x_{k,t_2,s}^j) - \tilde{\nabla} f_j(x_{k,t_2,s}^j) \right], \sum_{j \in C^{\ell_i}} \left\{ Q_1^{(\alpha)} \left[\sum_{\beta=0}^{\tau_1-1} \tilde{\nabla} f_j(x_{k,\alpha,\beta}^j) \right] - \sum_{\beta=0}^{\tau_1-1} \nabla f(x_{k,\alpha,\beta}^j) \right\} \right\rangle \\ &= \mathbb{E}_{x_{k,t_2,s}^j, \{x_{k,\alpha,\beta}^j\}_{\beta=0}^{\tau_1}, \{\xi_{k,\alpha,\beta}^j\}_{\beta=0}^{\tau_1}} \left\langle 0, \sum_{j \in C^{\ell_i}} \left\{ Q_1^{(\alpha)} \left[\sum_{\beta=0}^{\tau_1-1} \tilde{\nabla} f_j(x_{k,\alpha,\beta}^j) \right] - \sum_{\beta=0}^{\tau_1-1} \nabla f(x_{k,\alpha,\beta}^j) \right\} \right\rangle = 0 \end{aligned}$$

$$3) \forall s < t, \mathbb{E} \left\langle \sum_{j \in C^{\ell_i}} \left\{ \mathcal{Q}_1^{(\alpha)} \left[\sum_{\beta=0}^{\tau_1-1} \tilde{\nabla} f_j(x_{k,s,\beta}^j) \right] - \sum_{\beta=0}^{\tau_1-1} \nabla f(x_{k,s,\beta}^j) \right\}, \sum_{j \in C^{\ell_i}} \left\{ \mathcal{Q}_1^{(\alpha)} \left[\sum_{\beta=0}^{\tau_1-1} \tilde{\nabla} f_j(x_{k,t,\beta}^j) \right] - \sum_{\beta=0}^{\tau_1-1} \nabla f(x_{k,t,\beta}^j) \right\} \right\rangle.$$

The expansion of this form of inner product is very complex, but it can still be proved to be 0 in the expectation following the same idea of using the conditional independence as in the previous two examples.

Now we continue to bound the three terms A, B_1, B_2 in (41).

$$A \leq t_1 \sum_{\beta=0}^{t_1-1} \mathbb{E} \|\nabla f(x_{k,t_2,\beta})\|^2 + \frac{1}{m^{\ell_i}} t_2 \tau_1 \sum_{i \in C_i^{\ell}} \sum_{\alpha=0}^{t_2-1} \sum_{\beta=0}^{\tau_1-1} \mathbb{E} \|\nabla f(x_{k,\alpha,\beta}^j)\|^2 \quad (42)$$

$$B_1 = \sum_{\beta=0}^{t_1-1} \mathbb{E} \left\| \left[\tilde{\nabla} f_i(x_{k,t_2,\beta}^i) - \nabla f(x_{k,t_2,\beta}^i) \right] \right\|^2 \leq t_1 \sigma^2 \quad (43)$$

(43) directly comes from Assumption 2.

$$B_2 = \sum_{\alpha=0}^{t_2-1} \mathbb{E} \left\| \sum_{j \in C^{\ell_i}} \frac{1}{m^{\ell_i}} \left\{ \mathcal{Q}_1^{(\alpha)} \left[\sum_{\beta=0}^{\tau_1-1} \tilde{\nabla} f_j(x_{k,\alpha,\beta}^j) \right] - \sum_{\beta=0}^{\tau_1-1} \nabla f(x_{k,\alpha,\beta}^j) \right\} \right\|^2 \quad (44)$$

$$= \sum_{\alpha=0}^{t_2-1} \sum_{j \in C^{\ell_i}} \frac{1}{(m^{\ell_i})^2} \mathbb{E} \left\| \left\{ \mathcal{Q}_1^{(\alpha)} \left[\sum_{\beta=0}^{\tau_1-1} \tilde{\nabla} f_j(x_{k,\alpha,\beta}^j) \right] - \sum_{\beta=0}^{\tau_1-1} \nabla f(x_{k,\alpha,\beta}^j) \right\} \right\|^2 \quad (45)$$

$$= \sum_{\alpha=0}^{t_2-1} \sum_{j \in C^{\ell_i}} \frac{1}{(m^{\ell_i})^2} \mathbb{E} \left\| \left\{ \mathcal{Q}_1^{(\alpha)} \left[\sum_{\beta=0}^{\tau_1-1} \tilde{\nabla} f_j(x_{k,\alpha,\beta}^j) \right] - \sum_{\beta=0}^{\tau_1-1} \tilde{\nabla} f_j(x_{k,\alpha,\beta}^j) \right\} \right\|^2 + \left\| \left\{ \sum_{\beta=0}^{\tau_1-1} \tilde{\nabla} f_j(x_{k,\alpha,\beta}^j) - \sum_{\beta=0}^{\tau_1-1} \nabla f(x_{k,\alpha,\beta}^j) \right\} \right\|^2 \right\} \quad (46)$$

$$\leq \sum_{\alpha=0}^{t_2-1} \sum_{j \in C^{\ell_i}} \frac{1}{(m^{\ell_i})^2} \left\{ q_1 \mathbb{E} \left\| \sum_{\beta=0}^{\tau_1-1} \tilde{\nabla} f_j(x_{k,\alpha,\beta}^j) \right\|^2 + \tau_1 \sigma^2 \right\} \quad (47)$$

$$\leq \sum_{\alpha=0}^{t_2-1} \sum_{j \in C^{\ell_i}} \frac{1}{(m^{\ell_i})^2} \left\{ q_1 \mathbb{E} \left\| \sum_{\beta=0}^{\tau_1-1} \nabla f(x_{k,\alpha,\beta}^j) \right\|^2 + q_1 \tau_1 \sigma^2 \right\} + \frac{1}{m^{\ell_i}} t_2 \tau_1 \sigma^2 \quad (48)$$

$$\leq \sum_{\alpha=0}^{t_2-1} \sum_{j \in C^{\ell_i}} \frac{1}{(m^{\ell_i})^2} \left\{ q_1 \tau_1 \sum_{\beta=0}^{\tau_1-1} \mathbb{E} \|\nabla f(x_{k,\alpha,\beta}^j)\|^2 \right\} + \frac{1+q_1}{m^{\ell_i}} t_2 \tau_1 \sigma^2 \quad (49)$$

Now we can write the bound on (36):

$$\mathbb{E} \left\| \nabla f(x_k) - \nabla f(x_{k,t_2,t_1}^j) \right\|^2 \leq L^2 \eta^2 (A + B_1 + B_2) \quad (50)$$

$$\leq L^2 \eta^2 \left\{ \underbrace{t_1 \sum_{\beta=0}^{t_1-1} \mathbb{E} \|\nabla f(x_{k,t_2,\beta})\|^2 + \frac{1}{m^{\ell_i}} \left(t_2 \tau_1 + \frac{q_1 \tau_1}{m^{\ell_i}} \right) \sum_{i \in C_i^{\ell}} \sum_{\alpha=0}^{t_2-1} \sum_{\beta=0}^{\tau_1-1} \mathbb{E} \|\nabla f(x_{k,\alpha,\beta}^j)\|^2}_{C_1} \right\} + L^2 \eta^2 \left\{ \underbrace{t_1 \sigma^2 + \frac{1+q_1}{m^{\ell_i}} t_2 \tau_1 \sigma^2}_{C_2} \right\} \quad (51)$$

Then summing C_1 over i, t_2, t_1 :

$$\frac{1}{n} \sum_{i=1}^n \sum_{t_2=0}^{\tau_2-1} \sum_{t_1=0}^{\tau_1-1} C_1 \quad (52)$$

$$= \frac{1}{n} \sum_{i=1}^n \sum_{t_2=0}^{\tau_2-1} \sum_{t_1=0}^{\tau_1-1} \left(t_1 \sum_{\beta=0}^{t_1-1} \mathbb{E} \|\nabla f(x_{k,t_2,\beta})\|^2 + \frac{1}{m^{\ell_i}} \left(t_2 \tau_1 + \frac{q_1 \tau_1}{m^{\ell_i}} \right) \sum_{j \in \mathcal{C}_i^{\ell}} \sum_{\alpha=0}^{t_2-1} \sum_{\beta=0}^{\tau_1-1} \mathbb{E} \|\nabla f(x_{k,\alpha,\beta}^j)\|^2 \right) \quad (53)$$

$$\leq \frac{(\tau_1 - 1) \tau_1}{2} \frac{1}{n} \sum_{i=1}^n \sum_{\alpha=0}^{\tau_2-1} \sum_{\beta=0}^{\tau_1-1} \mathbb{E} \|\nabla f(x_{k,t_2,\beta})\|^2 + \frac{1}{n} \sum_{i=1}^n \sum_{t_2=0}^{\tau_2-1} \sum_{t_1=0}^{\tau_1-1} (t_2 \tau_1 + q_1 \tau_1) \frac{1}{m^{\ell_i}} \sum_{j \in \mathcal{C}_i^{\ell}} \sum_{\alpha=0}^{\tau_2-1} \sum_{\beta=0}^{\tau_1-1} \mathbb{E} \|\nabla f(x_{k,\alpha,\beta}^j)\|^2 \quad (54)$$

$$= \frac{(\tau_1 - 1) \tau_1}{2} \frac{1}{n} \sum_{i=1}^n \sum_{\alpha=0}^{\tau_2-1} \sum_{\beta=0}^{\tau_1-1} \mathbb{E} \|\nabla f(x_{k,t_2,\beta})\|^2 + \frac{1}{n} \sum_{i=1}^n \frac{1}{m^{\ell_i}} \sum_{j \in \mathcal{C}_i^{\ell}} \sum_{\alpha=0}^{\tau_2-1} \sum_{\beta=0}^{\tau_1-1} \mathbb{E} \|\nabla f(x_{k,\alpha,\beta}^j)\|^2 \times \sum_{t_2=0}^{\tau_2-1} \sum_{t_1=0}^{\tau_1-1} (t_2 \tau_1 + q_1 \tau_1) \quad (55)$$

$$= \frac{(\tau_1 - 1) \tau_1}{2} \frac{1}{n} \sum_{i=1}^n \sum_{\alpha=0}^{\tau_2-1} \sum_{\beta=0}^{\tau_1-1} \mathbb{E} \|\nabla f(x_{k,\alpha,\beta})\|^2 + \frac{1}{n} \sum_{i=1}^n \sum_{\alpha=0}^{\tau_2-1} \sum_{\beta=0}^{\tau_1-1} \mathbb{E} \|\nabla f(x_{k,\alpha,\beta}^i)\|^2 \times \tau_1 \tau_2 \left(\frac{\tau_1(\tau_2 - 1)}{2} + q_1 \tau_2 \right) \quad (56)$$

$$= \left[\frac{(\tau_1 - 1) \tau_1}{2} + \tau_1 \tau_2 \left(\frac{\tau_1(\tau_2 - 1)}{2} + q_1 \tau_2 \right) \right] \frac{1}{n} \sum_{i=1}^n \sum_{\alpha=0}^{\tau_2-1} \sum_{\beta=0}^{\tau_1-1} \mathbb{E} \|\nabla f(x_{k,\alpha,\beta})\|^2 \quad (57)$$

Summing C_2 over i, t_2, t_1 :

$$\frac{1}{n} \sum_{i=1}^n \sum_{t_2=0}^{\tau_2-1} \sum_{t_1=0}^{\tau_1-1} C_2 = \frac{1}{n} \sum_{i=1}^n \sum_{t_2=0}^{\tau_2-1} \sum_{t_1=0}^{\tau_1-1} \left(t_1 \sigma^2 + \frac{1+q_1}{m^{\ell_i}} t_2 \tau_1 \sigma^2 \right) = \frac{\tau_1 \tau_2}{2} \left((\tau_1 - 1) + \frac{s}{n} (1 + q_1) \tau_1 (\tau_2 - 1) \right) \sigma^2 \quad (58)$$

Finally, we derive the upper bound in the Lemma 2:

$$\mathbb{E} \langle \nabla f(x_k), \bar{x}_{k+1} - x_k \rangle \quad (59)$$

$$\begin{aligned} &\leq -\frac{\eta}{2} \sum_{j \in [n]} \frac{1}{n} \sum_{t_2=0}^{\tau_2-1} \sum_{t_1=0}^{\tau_1-1} \mathbb{E} \|\nabla f(x_k)\|^2 - \frac{\eta}{2} \sum_{j \in [n]} \frac{1}{n} \sum_{t_2=0}^{\tau_2-1} \sum_{t_1=0}^{\tau_1-1} \mathbb{E} \|\nabla f(x_{k,t_2,t_1}^i)\|^2 + \frac{L^2 \eta^3}{2} \sum_{j \in [n]} \frac{1}{n} \sum_{t_2=0}^{\tau_2-1} \sum_{t_1=0}^{\tau_1-1} (C_1 + C_2) \\ &\leq -\frac{\eta}{2} \sum_{j \in [n]} \frac{1}{n} \sum_{t_2=0}^{\tau_2-1} \sum_{t_1=0}^{\tau_1-1} \mathbb{E} \|\nabla f(x_k)\|^2 - \frac{\eta}{2} \sum_{j \in [n]} \frac{1}{n} \sum_{t_2=0}^{\tau_2-1} \sum_{t_1=0}^{\tau_1-1} \mathbb{E} \|\nabla f(x_{k,t_2,t_1}^i)\|^2 \\ &\quad + \frac{L^2 \eta^3}{2} \left\{ \left[\frac{(\tau_1 - 1) \tau_1}{2} + \tau_1 \tau_2 \left(\frac{\tau_1(\tau_2 - 1)}{2} + q_1 \tau_2 \right) \right] \frac{1}{n} \sum_{i=1}^n \sum_{\alpha=0}^{\tau_2-1} \sum_{\beta=0}^{\tau_1-1} \mathbb{E} \|\nabla f(x_{k,\alpha,\beta}^i)\|^2 \right\} \\ &\quad + \frac{L^2 \eta^3}{2} \frac{\tau_1 \tau_2}{2} \left[(\tau_1 - 1) + \frac{s}{n} (1 + q_1) \tau_1 (\tau_2 - 1) \right] \sigma^2 \end{aligned} \quad (60)$$

$$\begin{aligned} &\leq -\frac{\eta}{2} \tau_1 \tau_2 \mathbb{E} \|\nabla f(x_k)\|^2 - \frac{\eta}{2} \left\{ 1 - L^2 \eta^2 \left[\frac{\tau_1(\tau_1 - 1)}{2} + \tau_1 \tau_2 \left(\frac{\tau_2(\tau_2 - 1)}{2} + q_1 \tau_2 \right) \right] \right\} \frac{1}{n} \sum_{i=1}^n \sum_{\alpha=0}^{\tau_2-1} \sum_{\beta=0}^{\tau_1-1} \mathbb{E} \|\nabla f(x_{k,\alpha,\beta}^i)\|^2 \\ &\quad + \frac{L^2 \eta^3}{4} \tau_1 \tau_2 \left[(\tau_1 - 1) + \frac{s}{n} (1 + q_1) \tau_1 (\tau_2 - 1) \right] \sigma^2 \end{aligned} \quad (61)$$

□

Proof. Lemma 3: From Eqn. (10), using the property: $\mathbb{E}\|x\|^2 = \|\mathbb{E}x\|^2 + \text{Var}(x)^2$, we obtain:

$$\mathbb{E} \|\bar{x}_{k+1} - x_k\|^2 \quad (62)$$

$$= \eta^2 \mathbb{E} \left\| \frac{1}{n} \sum_{i \in [n]} \sum_{t_2=0}^{\tau_2-1} \mathcal{Q}_1^{(t_2)} \left[\sum_{t_1=0}^{\tau_1-1} \tilde{\nabla} f_i(x_{k,t_2,t_1}^i) \right] \right\|^2 \quad (63)$$

$$= \eta^2 \mathbb{E} \left\| \frac{1}{n} \sum_{i \in [n]} \sum_{t_2=0}^{\tau_2-1} \sum_{t_1=0}^{\tau_1-1} \nabla f(x_{k,t_2,t_1}^i) \right\|^2 + \eta^2 \frac{1}{n^2} \sum_{i \in [n]} \sum_{t_2=0}^{\tau_2-1} \mathbb{E} \left\| \mathcal{Q}_1^{(t_2)} \left[\sum_{t_1=0}^{\tau_1-1} \tilde{\nabla} f_i(x_{k,t_2,t_1}^i) \right] - \sum_{t_1=0}^{\tau_1-1} \nabla f(x_{k,t_2,t_1}^i) \right\|^2 \quad (64)$$

$$\leq \eta^2 \tau_1 \tau_2 \frac{1}{n} \sum_{i \in [n]} \sum_{t_2=0}^{\tau_2-1} \sum_{t_1=0}^{\tau_1-1} \mathbb{E} \|\nabla f(x_{k,t_2,t_1}^i)\|^2 + \eta^2 \frac{1}{n^2} \sum_{i \in [n]} \sum_{t_2=0}^{\tau_2-1} \left\{ q_1 \mathbb{E} \left\| \sum_{t_1=0}^{\tau_1-1} \nabla f(x_{k,t_2,t_1}^i) \right\|^2 + (1+q_1)\tau_1\sigma^2 \right\} \quad (65)$$

$$= \eta^2 \left(\tau_1 \tau_2 + \frac{q_1 \tau_1}{n} \right) \frac{1}{n} \sum_{i=1}^n \sum_{\alpha=0}^{\tau_2-1} \sum_{\beta=0}^{\tau_1-1} \mathbb{E} \|\nabla f(x_{k,\alpha,\beta}^i)\|^2 + \eta^2 \frac{1}{n} (1+q_1)\tau_1\tau_2\sigma^2 \quad (66)$$

□

Proof. Lemma 4: From Eqn. (10), (11), we know that:

$$E \|x_{k+1} - \bar{x}_{k+1}\|^2 = \eta^2 \mathbb{E} \left\| \sum_{\ell \in [s]} \frac{m^\ell}{n} \left\{ \mathcal{Q}_2 \left[\frac{1}{m^\ell} \sum_{\alpha=0}^{\tau_2-1} \sum_{j \in C^\ell} \mathcal{Q}_1^{(\alpha)} \left(\sum_{\beta=0}^{\tau_1-1} \tilde{\nabla} f_j(x_{k,\alpha,\beta}^j) \right) \right] - \left[\frac{1}{m^\ell} \sum_{\alpha=0}^{\tau_2-1} \sum_{j \in C^\ell} \mathcal{Q}_1^{(\alpha)} \left(\sum_{\beta=0}^{\tau_1-1} \tilde{\nabla} f_j(x_{k,\alpha,\beta}^j) \right) \right] \right\} \right\|^2 \quad (67)$$

$$= \eta^2 \sum_{\ell \in [s]} \left(\frac{m^\ell}{n} \right)^2 q_2 \mathbb{E} \left\| \left[\frac{1}{m^\ell} \sum_{\alpha=0}^{\tau_2-1} \sum_{j \in C^\ell} \mathcal{Q}_1^{(\alpha)} \left(\sum_{\beta=0}^{\tau_1-1} \tilde{\nabla} f_j(x_{k,\alpha,\beta}^j) \right) \right] \right\|^2 \quad (68)$$

$$= \eta^2 \sum_{\ell \in [s]} \left(\frac{1}{n} \right)^2 q_2 \mathbb{E} \left\| \left[\sum_{\alpha=0}^{\tau_2-1} \sum_{j \in C^\ell} \mathcal{Q}_1^{(\alpha)} \left(\sum_{\beta=0}^{\tau_1-1} \tilde{\nabla} f_j(x_{k,\alpha,\beta}^j) \right) \right] \right\|^2 \quad (69)$$

By using $\mathbb{E}\|x\|^2 = \|\mathbb{E}x\|^2 + \text{Var}(x)^2$, and following a similar approach as the one in the proof of Lemma 3, we conclude:

$$E \|x_{k+1} - \bar{x}_{k+1}\|^2 \leq \eta^2 \sum_{\ell \in [s]} \left(\frac{1}{n} \right)^2 q_2 \left[\left(\tau_1 \tau_2 m^\ell + \tau_1 q_1 \right) \sum_{j \in C^\ell} \sum_{t_2=0}^{\tau_2-1} \sum_{t_1=0}^{\tau_1-1} \mathbb{E} \|\nabla f(x_{k,t_2,t_1}^j)\|^2 + m^\ell \tau_1 \tau_2 (1+q_1)\sigma^2 \right] \quad (70)$$

$$\leq \eta^2 \sum_{\ell \in [s]} \left(\frac{1}{n} \right)^2 q_2 \left[(\tau_1 \tau_2 n + \tau_1 q) \sum_{j \in C^\ell} \sum_{t_2=0}^{\tau_2-1} \sum_{t_1=0}^{\tau_1-1} \mathbb{E} \|\nabla f(x_{k,t_2,t_1}^j)\|^2 + m^\ell \tau_1 \tau_2 (1+q_1)\sigma^2 \right] \quad (71)$$

$$\leq \eta^2 q_2 \left(\tau_1 \tau_2 + \frac{q_1 \tau_1}{n} \right) \frac{1}{n} \sum_{i=1}^n \sum_{\alpha=0}^{\tau_2-1} \sum_{\beta=0}^{\tau_1-1} \mathbb{E} \|\nabla f(x_{k,\alpha,\beta}^i)\|^2 + \eta^2 \frac{1}{n} (1+q_1) q_2 \tau_1 \tau_2 \sigma^2 \quad (72)$$

□

REFERENCES

- [1] L. Liu, J. Zhang, S. H. Song, and K. B. Letaief, "Client-Edge-Cloud Hierarchical Federated Learning," in *2020 IEEE International Conference on Communications (ICC)*, 2020, pp. 1–6.
- [2] I. Goodfellow, Y. Bengio, and A. Courville, *Deep learning*, 2016.
- [3] B. McMahan, E. Moore, D. Ramage, S. Hampson, and B. A. y Arcas, "Communication-efficient learning of deep networks from decentralized data," in *Artificial Intelligence and Statistics*. PMLR, 2017, pp. 1273–1282.
- [4] A. Hard, K. Rao, R. Mathews, F. Beaufays, S. Augenstein, H. Eichner, C. Kiddon, and D. Ramage, "Federated learning for mobile keyboard prediction," *arXiv preprint arXiv:1811.03604*, 2018.
- [5] J. Konečný, H. B. McMahan, F. X. Yu, P. Richtárik, A. T. Suresh, and D. Bacon, "Federated learning: Strategies for improving communication efficiency," *arXiv preprint arXiv:1610.05492*, 2016.
- [6] A. Reisizadeh, A. Mokhtari, H. Hassani, A. Jadbabaie, and R. Pedarsani, "Fedpaq: A communication-efficient federated learning method with periodic averaging and quantization," in *International Conference on Artificial Intelligence and Statistics*, 2020, pp. 2021–2031.
- [7] N. H. Tran, W. Bao, A. Zomaya, N. M. NH, and C. S. Hong, "Federated learning over wireless networks: Optimization model design and analysis," in *IEEE INFOCOM 2019-IEEE Conference on Computer Communications*. IEEE, 2019, pp. 1387–1395.
- [8] S. Wang, T. Tuor, T. Salonidis, K. K. Leung, C. Makaya, T. He, and K. Chan, "Adaptive federated learning in resource constrained edge computing systems," *IEEE Journal on Selected Areas in Communications*, vol. 37, no. 6, pp. 1205–1221, 2019.
- [9] Y. Mao, C. You, J. Zhang, K. Huang, and K. B. Letaief, "A survey on mobile edge computing: The communication perspective," *IEEE Commun. Surveys Tuts.*, vol. 19, no. 4, pp. 2322–2358.
- [10] Y. Shi, K. Yang, T. Jiang, J. Zhang, and K. B. Letaief, "Communication-Efficient Edge AI: Algorithms and Systems," *IEEE Communications Surveys Tutorials*, vol. 22, no. 4, pp. 2167–2191, 2020.
- [11] G. Zhu, D. Liu, Y. Du, C. You, J. Zhang, and K. Huang, "Toward an Intelligent Edge: Wireless Communication Meets Machine Learning," *IEEE Communications Magazine*, vol. 58, no. 1, pp. 19–25, 2020.
- [12] J. Zhang and K. B. Letaief, "Mobile Edge Intelligence and Computing for the Internet of Vehicles," *Proceedings of the IEEE*, vol. 108, no. 2, pp. 246–261, 2020.
- [13] F. Zhou and G. Cong, "A distributed hierarchical SGD algorithm with sparse global reduction," *arXiv preprint arXiv:1903.05133*, 2019.
- [14] J. Wang, S. Wang, R.-R. Chen, and M. Ji, "Local Averaging Helps: Hierarchical Federated Learning and Convergence Analysis," *arXiv preprint arXiv:2010.12998*, 2020.
- [15] S. Luo, X. Chen, Q. Wu, Z. Zhou, and S. Yu, "HFEL: Joint Edge Association and Resource Allocation for Cost-Efficient Hierarchical Federated Edge Learning," *arXiv preprint arXiv:2002.11343*, 2020.
- [16] N. Mhaisen, A. Awad, A. Mohamed, A. Erbad, and M. Guizani, "Analysis and Optimal Edge Assignment For Hierarchical Federated Learning on Non-IID Data," *arXiv preprint arXiv:2012.05622*, 2020.
- [17] Y. LeCun and C. Cortes, "MNIST handwritten digit database," 2010. [Online]. Available: <http://yann.lecun.com/exdb/mnist/>
- [18] A. Krizhevsky *et al.*, "Learning multiple layers of features from tiny images," Citeseer, Tech. Rep., 2009.
- [19] L. Bottou, F. E. Curtis, and J. Nocedal, "Optimization methods for large-scale machine learning," *Siam Review*, vol. 60, no. 2, pp. 223–311, 2018.
- [20] S. U. Stich, "Local SGD Converges Fast and Communicates Little," in *ICLR 2019 ICLR 2019 International Conference on Learning Representations*, no. CONF, 2019.

- [21] A. Khaled, K. Mishchenko, and P. Richtárik, “Tighter theory for local SGD on identical and heterogeneous data,” in *International Conference on Artificial Intelligence and Statistics*. PMLR, 2020, pp. 4519–4529.
- [22] J. Wang and G. Joshi, “Cooperative SGD: A unified framework for the design and analysis of communication-efficient SGD algorithms,” *arXiv preprint arXiv:1808.07576*, 2018.
- [23] Y. Zhao, M. Li, L. Lai, N. Suda, D. Civin, and V. Chandra, “Federated learning with non-iid data,” *arXiv preprint arXiv:1806.00582*, 2018.
- [24] X. Li, K. Huang, W. Yang, S. Wang, and Z. Zhang, “On the Convergence of FedAvg on Non-IID Data,” in *International Conference on Learning Representations*, 2020. [Online]. Available: <https://openreview.net/forum?id=HJxNAnVtDS>
- [25] J. Wang and G. Joshi, “Adaptive Communication Strategies to Achieve the Best Error-Runtime Trade-off in Local-Update SGD,” in *Proceedings of Machine Learning and Systems*, A. Talwalkar, V. Smith, and M. Zaharia, Eds., vol. 1, 2019, pp. 212–229. [Online]. Available: <https://proceedings.mlsys.org/paper/2019/file/c8ffe9a587b126f152ed3d89a146b445-Paper.pdf>
- [26] M. Mohri, A. Rostamizadeh, and A. Talwalkar, *Foundations of machine learning*. MIT press, 2018.
- [27] S. U. Stich, J.-B. Cordonnier, and M. Jaggi, “Sparsified SGD with Memory,” *Advances in Neural Information Processing Systems*, vol. 31, pp. 4447–4458, 2018.
- [28] J. Liu, Y. Mao, J. Zhang, and K. B. Letaief, “Delay-optimal computation task scheduling for mobile-edge computing systems,” in *2016 IEEE International Symposium on Information Theory (ISIT)*, 2016, pp. 1451–1455.